

Dynamics of travelling breathers arising in reaction-diffusion systems — ODE modelling approach —

Masayasu MIMURA, Masaharu NAGAYAMA, Hideo IKEDA and
Tsutomu IKEDA

(Received June 4, 1999)

(Revised September 9, 1999)

ABSTRACT. We consider oscillatory travelling pulses with breathing motion, which are called travelling breathers, arising in a two-component bistable reaction-diffusion system with a small layer-parameter ε . Applying the interfacial dynamics procedure as $\varepsilon \downarrow 0$, we reduce the system to a 4-dimensional system of ODEs to describe the motion of front and back interfaces of the pulse. This reduction enables us to reveal the global structure of standing and travelling pulses as well as travelling breathers, by which qualitative properties of travelling breathers can be discussed.

1. Introduction

Theoretical understanding of a variety of spatio-temporal patterns in diffusive medium has been in progress by using several types of models of reaction-diffusion (RD) systems. Among them, mono-stable RD systems with excitability describe travelling pulses which correspond to action potential propagating along nerve fibers [7] or expanding rings or spiral waves in the Belousov-Zhabotinsky reactions [11]. It is well known that these travelling pulses and expanding rings stably exist.

However, recently, even if these are generated by mono-stable systems with excitability, it has been numerically observed that travelling pulses are not necessarily stable but move with oscillatory velocity [1], [5], [9], [10]. For example, Fig. 1.1 shows an oscillatory travelling pulse arising in the first step exothermic RD system [5].

As a prototype of RD systems which generate travelling pulses, there is the following FitzHugh-Nagumo type-system with a sufficiently small parameter $\delta > 0$ has been intensively investigated by many authors:

2000 *Mathematics Subject Classifications.* 35B25, 35B32, 35K57, 65C99.

Key words: bistable reaction-diffusion system, singular perturbation methods, travelling pulse, travelling breather.

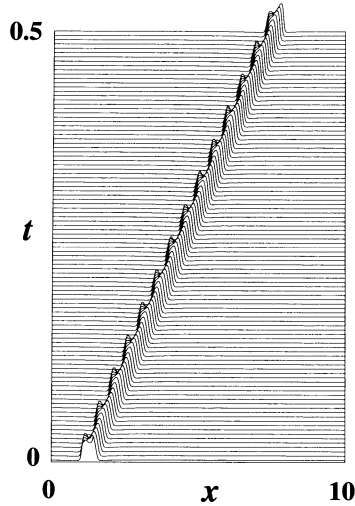


Fig. 1.1 Oscillatory propagating pulse of the exothermic RD system.

$$\begin{cases} \frac{\partial u}{\partial t} = d^{-1} \frac{\partial^2 u}{\partial x^2} + f(u) - v \\ \frac{\partial v}{\partial t} = \frac{\partial^2 v}{\partial x^2} + \delta(u - \gamma v). \end{cases} \quad t > 0, \quad x \in \mathbf{R} \quad (1.1)$$

Here $f(u)$ possesses cubic-like nonlinearity such as $f_c(u) = u(1-u)(u-a)$ or $f_{PL} = H(u-a) - u$ where $H(s) = 1$ for $s > 0$, $H(s) = 0$ for $s < 0$, $0 < a < 1/2$ and $\gamma (> 0)$ are both constants. When the kinetics in (1.1) takes suitable mono-stable property, there appear stable travelling pulses but no oscillatory travelling pulses. On the other hand, if (1.1) takes suitable bistable kinetics, it is numerically shown in [4] that there appear oscillatory travelling pulses when d is large, as in Fig. 1.2. A feature of these pulses is that the component u possesses one front- and one back-layers which move with breathing motion. We therefore call such pulse a *travelling breather*, and if it is motionless, a *standing breather*. One could expect that such travelling breathers appear as the consequence of Hopf bifurcation of travelling pulses, as in Fig. 1.3. However, we should note that travelling breathers do not necessarily persist, depending on values of parameters. Fig. 1.4 shows the extinction of travelling breather which develops from the travelling pulse, while Fig. 1.5 shows the transition from the travelling pulse to a standing breather where the pulse behaves as if it were a travelling breather in the transient process.

The aim of this paper is to understand how such dynamics of travelling breathers, as shown in Figs. 1.3–1.5, occurs.

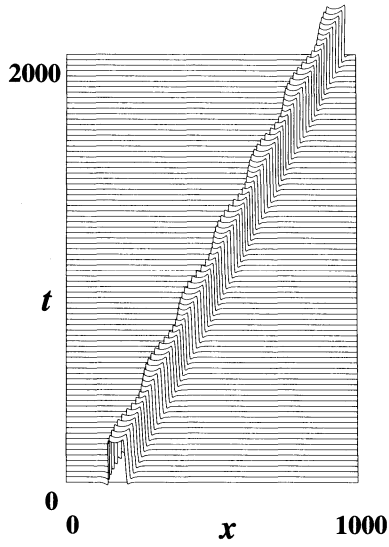


Fig. 1.2 Oscillatory propagating pulse (u -component) of (1.1) with $f(u) = u(1 - u)(u - a)$ where the parameters are $a = 0.25, \delta = 0.001, \gamma = 10.2, d = 2.12404$.

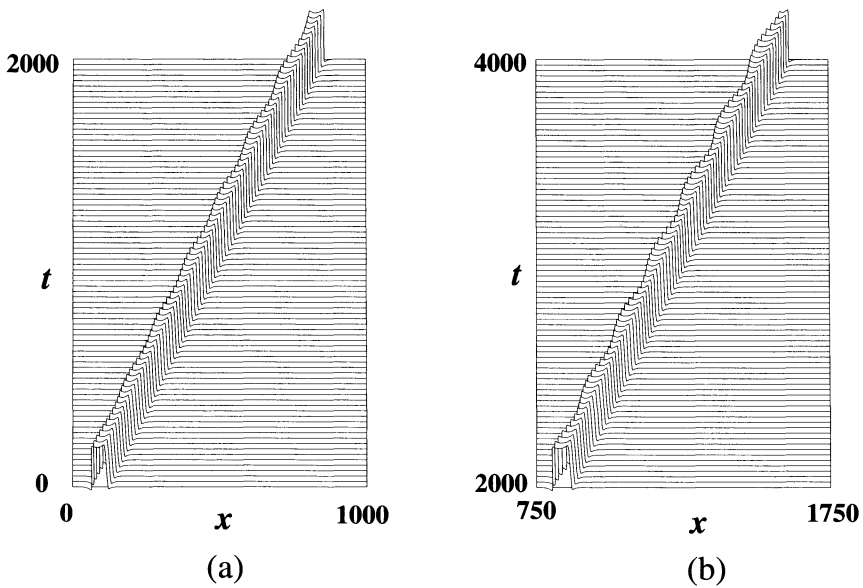


Fig. 1.3 Transition from the travelling pulse to a travelling breather in (1.1) where the parameters are the same as Fig. 1.2.

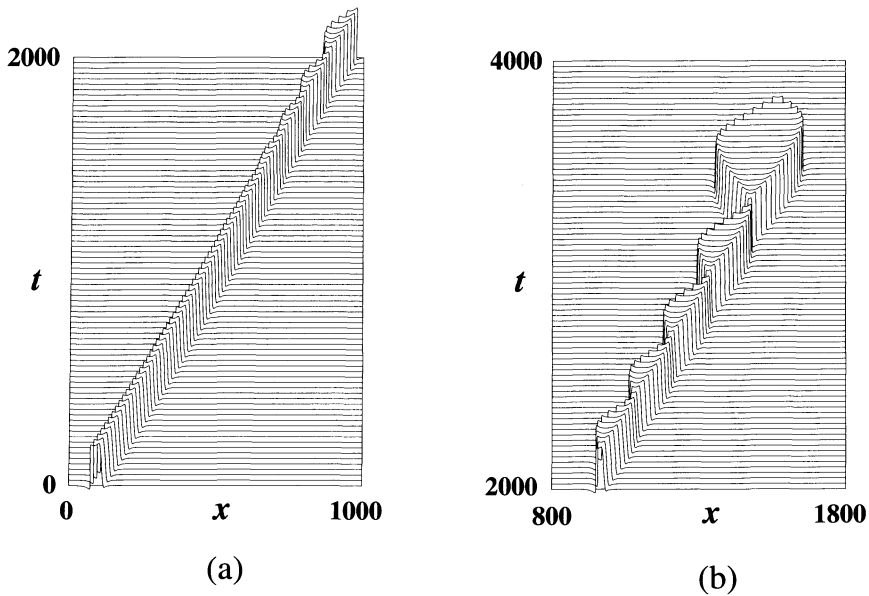


Fig. 1.4 Extinction of a travelling breather in (1.1) where the parameters are the same as Fig. 1.2 except $\gamma = 10.05$ and $d = 2.00080$.

In order to study this problem, we use $f_{PL}(u)$, which is known as a prototype of $f(u)$, in (1.1) and write it also as $f(u)$. This simplification of piecewise linearity reveals the global structure of travelling and standing pulses when d is varied. As d decreases, travelling pulses secondly bifurcating from the standing one at $d = d_T$ recover their stability through the Hopf bifurcation which occurs at $d = d_{TH}$, as in Fig. 1.6 (For bifurcation argument, see [3], [4]). This information strongly suggests that travelling breathers appear as a Hopf-bifurcation from the travelling pulse, although their existence and stability have been unsolved.

We derive a 4-dimensional system of ODEs from (1.1). The reduction is carried out in two processes; The first is to reduce (1.1) to a free boundary problem describing the dynamics of front and back interfaces coupled with v , and the second is to derive a 4-dimensional system of ODEs describing the front- and back-interfaces only from the free boundary problem. This system enables us to draw the structure of travelling pulses as well as travelling breathers when some parameter is varied, and gives some information on the dynamics of travelling breathers arising in (1.1) shown in Figs. 1.3–1.5.

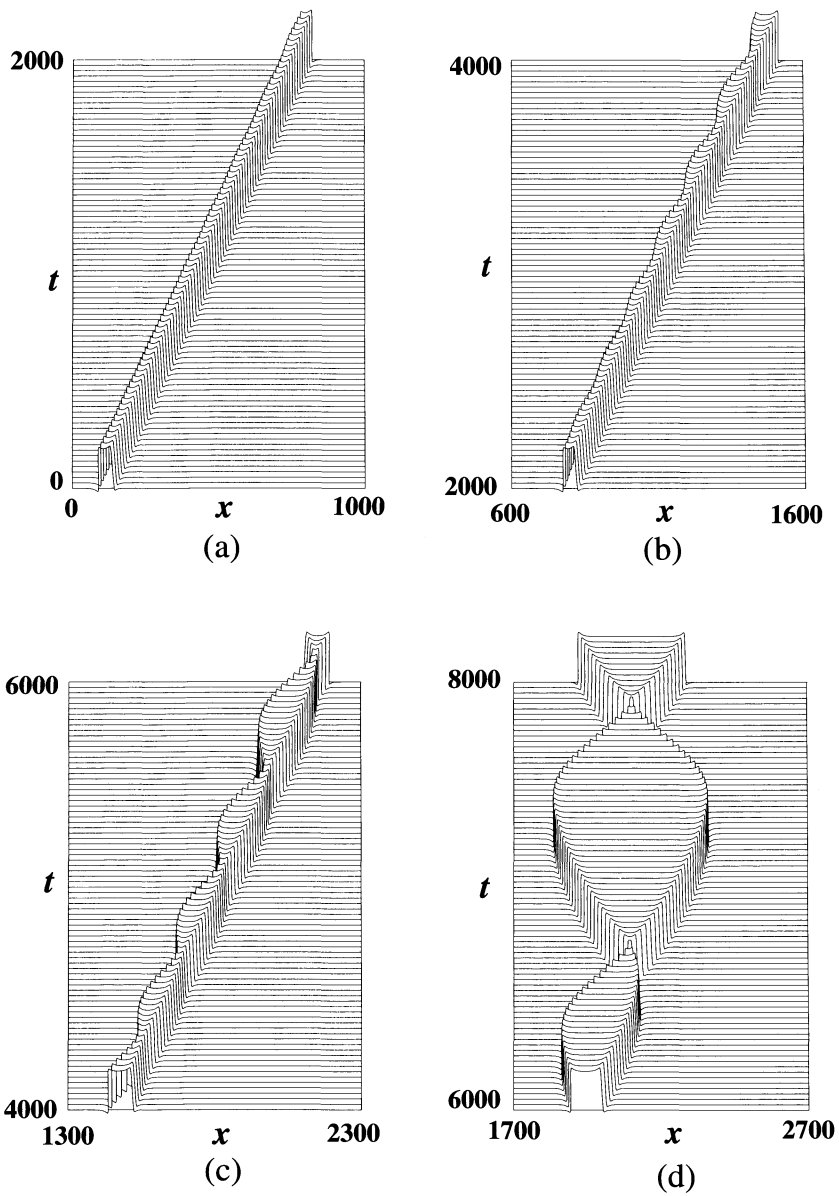


Fig. 1.5 Transition from the travelling pulse to a standing breather in (1.1) where the parameters are the same as Fig. 1.2 except $d = 2.12766$.

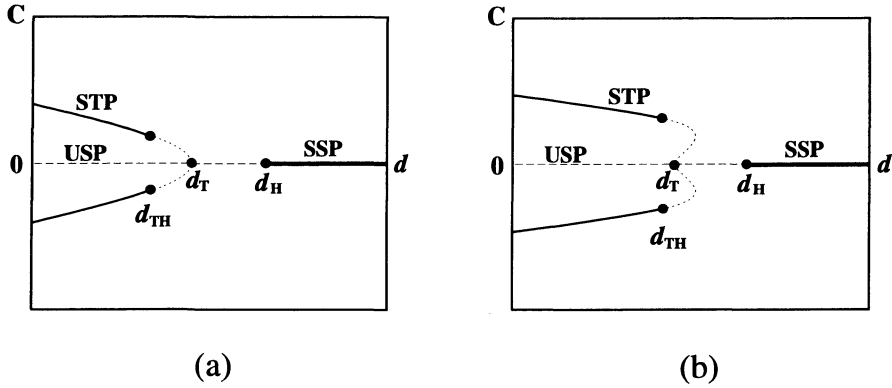


Fig. 1.6 Schematic bifurcation diagrams of standing and travelling pulses when the parameter d is varied, where the vertical axis indicates the velocity of the travelling pulse: (a) super-critical case; (b) sub-critical case. (SSP: stable standing pulse, USP: unstable standing pulse, STP: stable travelling pulse, d_H : Hopf bifurcation value of d with respect to the standing pulse, d_T : translational bifurcation value of d , d_{TH} : Hopf bifurcation value of d with respect to the travelling pulse.)

2. Limiting problem as $\varepsilon \downarrow 0$

By taking $\tau = \sqrt{\delta d}$ and $\varepsilon = \sqrt{\delta/d}$, we conveniently write (1.1) as

$$\begin{cases} \varepsilon \tau \frac{\partial u}{\partial t} = \varepsilon^2 \frac{\partial^2 u}{\partial x^2} + f(u) - v, \\ \frac{\partial v}{\partial t} = \frac{\partial^2 v}{\partial x^2} + u - \gamma v \end{cases} \quad t > 0, \quad x \in \mathbf{R}, \quad (2.1)$$

with the boundary conditions

$$\lim_{|x| \rightarrow \infty} (u, v)(t, x) = (0, 0). \quad (2.2)$$

We assume ε to be sufficiently small and take τ as a bifurcation parameter instead of d . We restrict ourselves to a single pulse-solution of (2.1), (2.2), where two internal layers appear in the u -component, as in Fig. 2.1(a). Taking the limit $\varepsilon \downarrow 0$ in (2.1), one can expect that these layers become interfaces, say $z_L(t)$ and $z_R(t)$, as in Fig. 2.1(b). By using the well known singular perturbation method ([12], for instance), the time-evolution for $z_L(t)$ and $z_R(t)$ ($-\infty < z_L(t) < z_R(t) < \infty$) can be approximately described by

$$\begin{cases} \tau \dot{z}_L = -\lambda(v(t, z_L(t))), \\ \tau \dot{z}_R = \lambda(v(t, z_R(t))), \end{cases} \quad t > 0, \quad (2.3)$$

where $\dot{\cdot}$ is the first derivative with time t and $\lambda(s)$ is given such that there is a bounded solution $w(x; s)$ to satisfy the following boundary value problem for

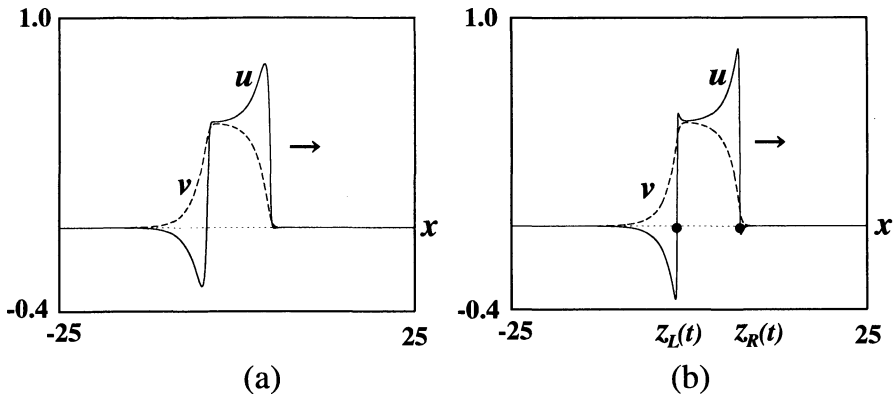


Fig. 2.1 Spatial profile of a pulse-solution of (2.1), (2.2): (a) $0 < \varepsilon \ll 1$; (b) $\varepsilon \downarrow 0$.

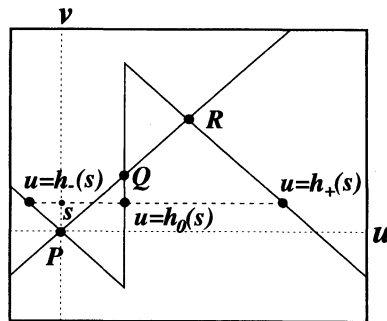


Fig. 2.2 The graph of $v = f(u)$, where $u = h_-(v)$, $u = h_+(v)$ and $u = h_0(v)$ denote three branches of $v = f(u)$.

fixed constant s

$$\begin{cases} \lambda w_x + w_{xx} + f(w) - s = 0, & x \in \mathbf{R}, \\ w(-\infty) = h_+(s) \quad \text{and} \quad w(+\infty) = h_-(s), \end{cases} \quad (2.4)$$

where $u = h_-(v)$ and $u = h_+(v)$ are given functions of v by the inverse of $v = f(u)$, as in Fig. 2.2. We note that the solution $(w(x; s), \lambda(s))$ of (2.4) is uniquely obtained, where $\lambda(s)$ is explicitly given by $\lambda(s) = (1 - 2a - 2s) / \sqrt{(a + s)(1 - a - s)}$. The values of v on the interfaces $x = z_L(t)$ and $x = z_R(t)$ are obtained by solving the equations

$$\begin{cases} \frac{\partial v}{\partial t} = \frac{\partial^2 v}{\partial x^2} + h_-(v) - \gamma v, & t > 0, \quad x \in \mathbf{R} \setminus (z_L(t), z_R(t)), \\ \frac{\partial v}{\partial t} = \frac{\partial^2 v}{\partial x^2} + h_+(v) - \gamma v, & t > 0, \quad x \in (z_L(t), z_R(t)) \end{cases} \quad (2.5)$$

with the boundary condition

$$\lim_{|x| \rightarrow \infty} v(t, x) = 0, \quad t > 0 \tag{2.6}$$

and the regularity condition

$$v(t, \cdot) \in C^1(\mathbf{R}), \quad t > 0. \tag{2.7}$$

For the derivation of (2.3)–(2.7), the reader should refer to [12], for instance. We note that (2.3)–(2.7) is a free boundary problem, where the interfaces $z_L(t)$ and $z_R(t)$ are free boundaries coupled with the unknown variable v . The convergence of (2.1), (2.2) to (2.3)–(2.7) as $\varepsilon \downarrow 0$ is discussed in [12].

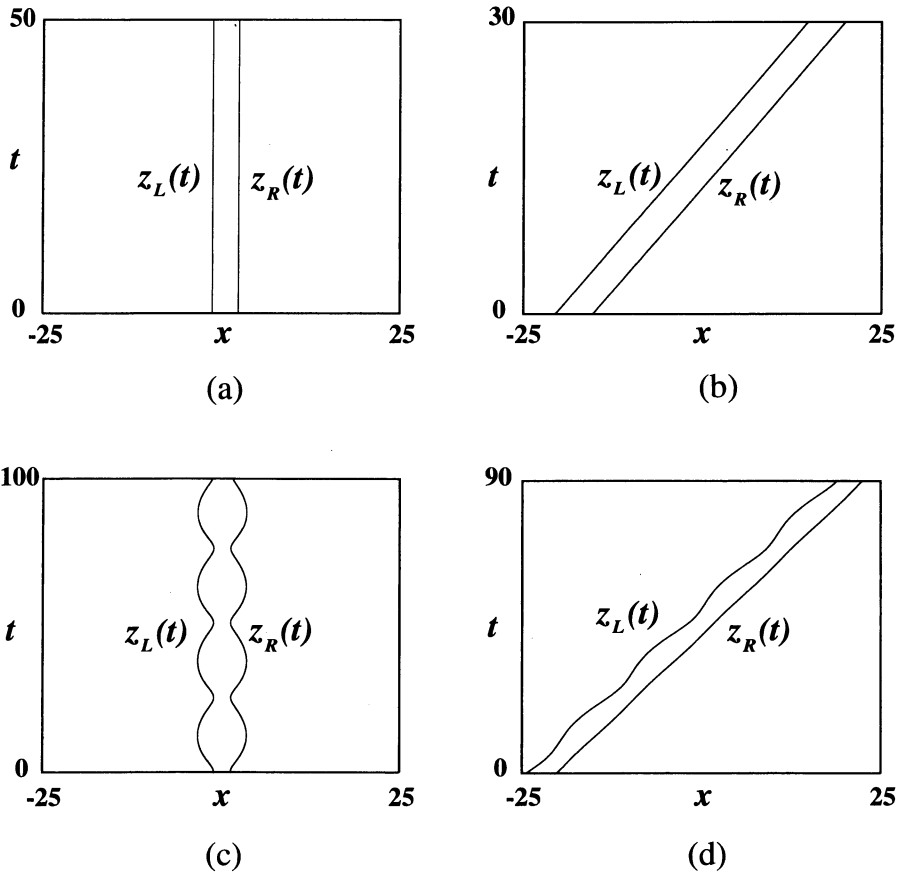


Fig. 2.3 Dynamics of interfaces $z_R(t)$ and $z_L(t)$ of (2.3)–(2.7) where the parameters are $a = 0.25, \gamma = 0.99$: (a) a standing interfaces ($\tau = 0.4$); (b) a travelling interfaces ($\tau = 0.33$); (c) a standing breather interfaces ($\tau = 0.358$); (d) a travelling breather interfaces ($\tau = 0.3432$).

With suitably fixed a and γ , four typical types of the interfaces $z_L(t)$ and $z_R(t)$ of (2.3)–(2.7) are shown in Figs. 2.3(a), (b), (c) and (d) for different values of τ , which correspond respectively to a standing pulse (SP), a travelling pulse (TP), a standing breather (SB) and a travelling breather (TB) arising in the RD system (2.1), (2.2). The $\varepsilon \downarrow 0$ limiting system (2.3)–(2.7) seems simpler than (2.1), (2.2), but it is still difficult to know the complete structure of SP-, TP-, SB- and TB-solutions when τ is varied.

3. 4-dimensional system of ODEs describing interfaces

The aim of this section is to derive a system ODEs describing two interfaces $x = z_L(t), z_R(t)$ from (2.3)–(2.7). We fix γ suitably close to γ^* but satisfy $\gamma < \gamma^*$, where $\gamma = \gamma^*$ is given such that P and R are odd symmetric with respect to Q , as in Fig. 2.2.

Assume that the interfaces $z_L(t)$ and $z_R(t)$ of the limiting problem (2.3)–(2.7) move very slowly. Then, applying the method in [6] to the limiting problem (2.3)–(2.7), we can formally obtain the following 4-dimensional system of ODEs describing the dynamics of $z_L(t)$ and $z_R(t)$:

$$\begin{cases} m(\dot{z}_L)\ddot{z}_L - n(z_R - z_L, -\dot{z}_R)\ddot{z}_R \\ \quad = -1 + 2a + M(z_R - z_L, -\dot{z}_L, -\dot{z}_R) - N(\dot{z}_L; \tau), \\ m(\dot{z}_R)\ddot{z}_R - n(z_R - z_L, \dot{z}_L)\ddot{z}_L \\ \quad = 1 - 2a - M(z_R - z_L, \dot{z}_R, \dot{z}_L) - N(\dot{z}_R; \tau), \end{cases} \tag{3.1}$$

where

$$m(p) = \frac{12}{\phi^5(p)}, \tag{3.2}$$

$$n(s, q) = \left(\frac{s^2}{\phi^3(q)} + \frac{6s}{\phi^4(q)} + \frac{12}{\phi^5(q)} \right) \exp(-s(\phi(q) + q)/2), \tag{3.3}$$

$$M(s, p, q) = \frac{\phi(p) - p}{\beta\phi(p)} - \frac{\phi(q) - q}{\beta\phi(q)} \exp(-s(\phi(q) + q)/2), \tag{3.4}$$

$$N(p; \tau) = \frac{\tau p}{\sqrt{((\tau p)^2 + 4)}} \tag{3.5}$$

with $\phi(k) = \sqrt{k^2 + 4\beta}$ and $\beta = 1 + \gamma$. The method and approximation used to derive (3.1) is shown in Appendix.

By introducing two new variables the center of two interfacial points, $x(t) = (z_R(t) + z_L(t))/2$ and the half length between them, $y(t) = (z_R(t) - z_L(t))/2$, it is convenient to rewrite (3.1) as

$$\begin{cases} \dot{x} = \xi, \\ 2A(\xi, 2y, \eta)\dot{\xi} = (m(\xi - \eta) + n(2y, -(\xi + \eta)))F_1(\xi, 2y, \eta; \tau) \\ \quad + (m(\xi + \eta) + n(2y, \xi - \eta))F_2(\xi, 2y, \eta; \tau), \\ \dot{y} = \eta, \\ 2A(\xi, 2y, \eta)\dot{\eta} = (m(\xi - \eta) - n(2y, -(\xi + \eta)))F_1(\xi, 2y, \eta; \tau) \\ \quad - (m(\xi + \eta) - n(2y, \xi - \eta))F_2(\xi, 2y, \eta; \tau), \end{cases} \quad (3.6)$$

where

$$A(p, s, q) = m(p - q)m(p + q) - n(s, -p - q)n(s, p - q), \quad (3.7)$$

$$F_1(p, s, q; \tau) = 1 - 2a - M(s, p + q, p - q) - N(p + q; \tau), \quad (3.8)$$

$$F_2(p, s, q; \tau) = -1 + 2a + M(s, -p + q, -p - q) - N(p - q; \tau). \quad (3.9)$$

Here we note that $A(p, s, q) > 0$ for any $s (> 0)$, p and q and $A(p, 0, q) = 0$, that is, as far as $y > 0$ holds, the system (3.6) is not degenerate. Since the variable x is not included in (3.6), which implies the translation free of interfaces in space, (3.6) essentially reduces to the following three-component system for the unknown variables ξ, y and η :

$$\begin{cases} \dot{\xi} = F(\xi, y, \eta; \tau), \\ \dot{y} = \eta, \\ \dot{\eta} = G(\xi, y, \eta; \tau), \end{cases} \quad t > 0, \quad (3.10)$$

where

$$\begin{cases} F(\xi, y, \eta; \tau) = \frac{1}{2A(\xi, 2y, \eta)} [(m(\xi - \eta) + n(2y, -\xi - \eta))F_1(\xi, 2y, \eta; \tau) \\ \quad + (m(\xi + \eta) + n(2y, \xi - \eta))F_2(\xi, 2y, \eta; \tau)], \\ G(\xi, y, \eta; \tau) = \frac{1}{2A(\xi, 2y, \eta)} [(m(\xi - \eta) - n(2y, -\xi - \eta))F_1(\xi, 2y, \eta; \tau) \\ \quad - (m(\xi + \eta) - n(2y, \xi - \eta))F_2(\xi, 2y, \eta; \tau)]. \end{cases} \quad (3.11)$$

For the system (3.10), we have to require $y(t) > 0$, that is, $z_R(t) > z_L(t)$ for any $t > 0$. If there is some $t_1 > 0$ such that $y(t) > 0$ for $0 < t < t_1$ and $y(t_1) = 0$, we may say that the pulse becomes extinction at $t = t_1$, while it expands to infinity, if $y(t)$ tends to infinity, as t goes on.

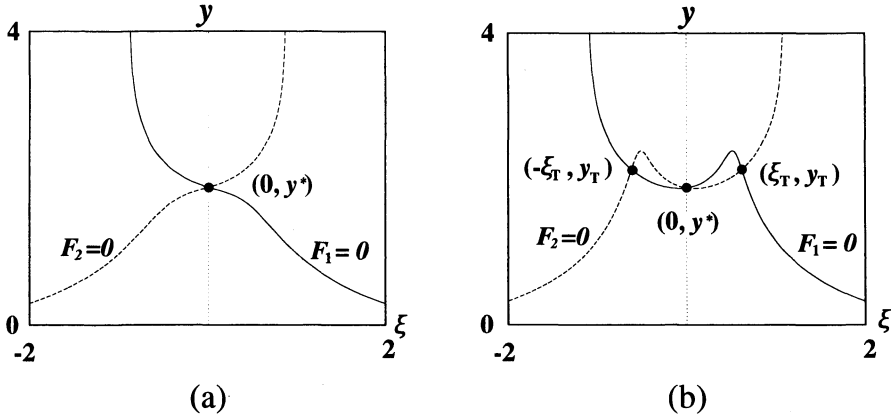


Fig. 3.1 Curves of $F_1 = 0$ and $F_2 = 0$ in (ξ, y) -plane: (a) τ is large; (b) τ is small.

By Fig. 3.1, we find that the trivial critical point is $(\xi, y, \eta) = (0, y^*, 0)$ with $y^* = -\sqrt{1/4\beta} \log(2a\beta + 1 - \beta)$, which is independent of $\tau > 0$. This indicates that $(x, \xi, y, \eta) = (x^*, 0, y^*, 0)$ is an equilibrium solution of (3.6) for arbitrarily fixed $x^* \in \mathbf{R}$, which corresponds to an SP-interfaces solution with the pulse-length $2y^*$ of the limiting problem (2.3)–(2.7), where the arbitrariness of x^* indicates translation free. We thus call $(0, y^*, 0)$ an SP-critical point of (3.10). The other is of the form $(\xi, y, \eta) = (\pm \xi_T, y_T, 0)$ with $\xi_T > 0$, which bifurcate from $(0, y^*, 0)$ when τ decreases. The corresponding $(x^* \pm \xi_T t, \xi_T, y_T, 0)$ are solutions of (3.6), which give TP-interfaces solutions of (2.3)–(2.7) where the velocity are $\pm \xi_T$ and the pulse-length is $2y_T$. We thus call $(\pm \xi_T, y_T, 0)$ TP-critical points of (3.10). Furthermore, suppose that (3.10) has a periodic solution $(\xi_0(t), y_0(t), \eta_0(t))$ with period θ . If $\xi_0(t) \equiv 0$, it corresponds to an SB-interfaces solution of (2.3)–(2.7). Writing $\xi_0(t)$ as $\xi_0(t) = \bar{\xi} + \xi_1(t)$ where $\bar{\xi}$ is the averaged value of $\xi_0(t)$ and $\xi_1(t)$ is a periodic function with $\int_0^\theta \xi_1(s) ds = 0$, we find that $(x^* + \bar{\xi}t + \int_0^t \xi_1(s) ds, \bar{\xi} + \xi_1(t), y_0(t), \eta_0(t))$ is a solution of (3.6) where $\int_0^t \xi_1(s) ds, \xi_1(t), y_0(t)$ and $\eta_0(t)$ are all periodic functions with period θ . This implies a TB-interfaces solution of (2.3)–(2.7). We thus call $(\xi_0(t), y_0(t), \eta_0(t))$ a TB-periodic solution and particularly, if $\xi_0(t) \equiv 0$, it is an SB-periodic one of (3.10). The existence of periodic solutions of (3.10) will be discussed in the next section.

We define the stability of these solutions.

DEFINITION 3.1. *Let $(\xi_T, y_T, 0)$ be a TP-critical point of (3.10), and let $(x(t), \xi(t), y(t), \eta(t))$ be a solution of (3.6) with the initial condition $(x(0), \xi(0), y(0), \eta(0))$. Then $(x^* + \xi_T t, \xi_T, y_T, 0)$ with any fixed $x^* \in \mathbf{R}$ is*

exponentially stable if there exists some constant $\delta > 0$ such that under the conditions,

$$|\xi(0) - \xi_T| < \delta, \quad |y(0) - y_T| < \delta, \quad |\eta(0)| < \delta, \quad (3.12)$$

there exist some constants $h, C_1 > 0$ and $C_2 > 0$ such that

$$\lim_{t \rightarrow \infty} [x(t) - (x^* + \xi_T t)] = h \quad (3.13)$$

and

$$|\xi(t) - \xi_T| + |y(t) - y_T| + |\eta(t)| < C_1 \exp(-C_2 t). \quad (3.14)$$

Stability of SP-interfaces solutions is similarly defined.

DEFINITION 3.2. Let $(\xi_0(t), y_0(t), \eta_0(t))$ be a TB-periodic solution with period θ of (3.10), and let $(x(t), \xi(t), y(t), \eta(t))$ be a solution of (3.6) with the initial condition $(x(0), \xi(0), y(0), \eta(0))$. Then $(x^* + \int_0^t \xi_0(s) ds, \xi_0(t), y_0(t), \eta_0(t))$ for any fixed $x^* \in \mathbf{R}$ is exponentially stable if there exists some constant $\delta > 0$ such that under the condition,

$$\begin{aligned} \min_{t \in [0, \theta]} |\xi(0) - \xi_0(t)| < \delta, \quad \min_{t \in [0, \theta]} |y(0) - y_0(t)| < \delta, \\ \min_{t \in [0, \theta]} |\eta(0) - \eta_0(t)| < \delta, \end{aligned} \quad (3.15)$$

there exist some constants $h, C_1 > 0, C_2 > 0$ and $\theta_0 \in (0, \theta)$ such that

$$\lim_{t \rightarrow \infty} \left[x(t) - \left(x^* + \int_0^{t+\theta_0} \xi_0(s) ds \right) \right] = h \quad (3.16)$$

and

$$|\xi(t) - \xi_0(t + \theta_0)| + |y(t) - y_0(t + \theta_0)| + |\eta(t) - \eta_0(t + \theta_0)| < C_1 \exp(-C_2 t). \quad (3.17)$$

We will find in Appendix that the stability of SP- and TP-critical points and SB- and TB-periodic solutions of (3.10) is inherited to the corresponding solutions of (3.6).

4. Global structure of pulse-solutions to the ODEs

In this section, we fix $a = 0.25$, and numerically draw the structures of critical points and periodic solutions of the 3-dimensional system of ODEs (3.10) when τ is globally varied.

We first consider the structures of SP-critical points and SB-periodic solutions of (3.10). Because of $\xi = 0$, these can be obtained by solving the

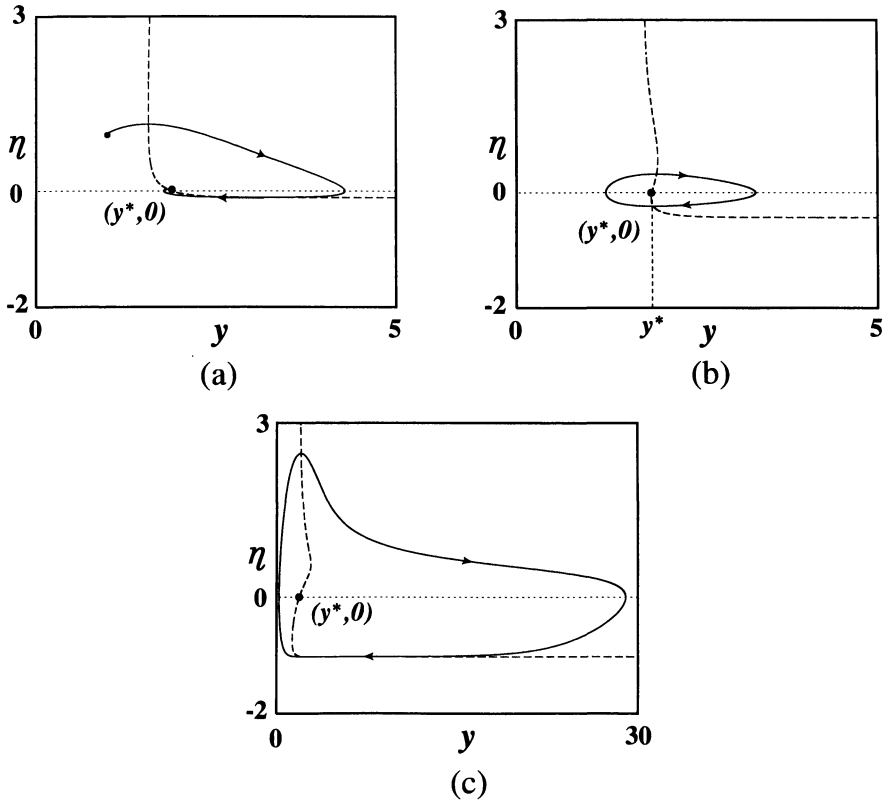


Fig. 4.1 Nulclines $g(y, \eta; \tau) = 0$ and solution-trajectories of (4.1) in (y, η) -plane where $a = 0.25, \beta = 1.99$: (a) $\tau = 0.4$; (b) $\tau = 0.365$; (c) $\tau = 0.345$.

following 2-dimensional system for y and η :

$$\begin{cases} \dot{y}(t) = \eta, \\ \dot{\eta}(t) = G(0, y, \eta; \tau) \equiv g(y, \eta; \tau), \end{cases} \quad (4.1)$$

where

$$g(y, \eta; \tau) = \frac{1}{m(\eta) + n(2y, -\eta)} \{1 - 2a - M(2y, \eta, -\eta) - N(\eta; \tau)\}. \quad (4.2)$$

We note that (4.1) is valid even if y takes negative, though it loses the meaning of the pulse-length. For different values of τ , solution-trajectories of (4.1) are drawn in Fig. 4.1, where $(y, \eta) = (y^*, 0)$ is the unique critical point. There is the critical value, say $\tau = \tau_H$, so that an SB-periodic solution $(y_0(t; \tau), \eta_0(t; \tau))$

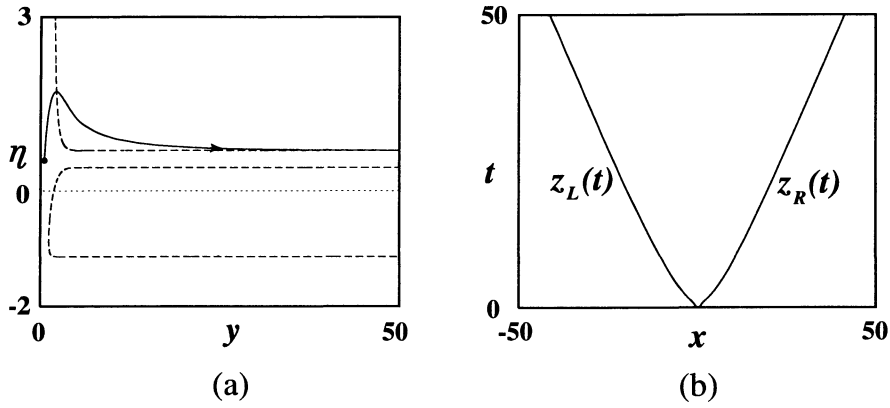


Fig. 4.2 (a) A solution-trajectory of (4.1); (b) the corresponding interfaces where the parameters are the same as Fig. 4.1 except $\tau = 0.341$.

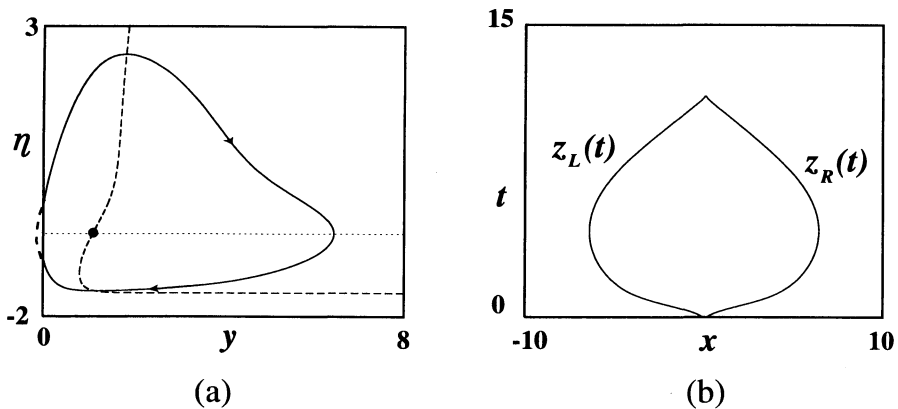


Fig. 4.3 (a) A limit cycle of (4.1) with negative value $y(t)$; (b) the corresponding interfaces where the parameters are the same as Fig. 4.1 except $\tau = 0.39$ and $\gamma = 0.9$.

is bifurcated from $(y^*, 0)$ for $\tau < \tau_H$, where the kinetics of (4.1) is qualitatively similar to that of the well-known Van der Pol equations.

As τ decreases from τ_H , we note that the SB-periodic solution disappears at one of two critical values at which $y_0(t; \tau)$ tends to infinity: One is $\tau_{H\infty}$ where it tends to infinity as t increases to infinity (Fig. 4.2). The other is τ_{H-} where it tends to zero after finite time (Fig. 4.3). When τ is larger but close to $\tau_{H\infty}$, $y_0(t; \tau)$ oscillates with very large amplitude and the corresponding $z_L(t)$

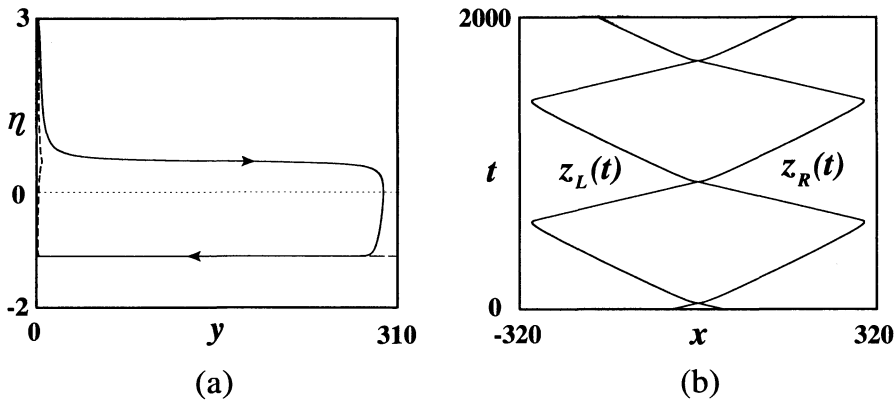


Fig. 4.4 (a) A limit cycle of (4.1); (b) the corresponding SB-interfaces where the parameters are the same as Fig. 4.1 except $\tau = 0.34205$.

and $z_R(t)$ take saw-toothed shape, as if they move with piecewise constant velocity, as in Fig. 4.4.

The velocity is approximately determined as follows: Introducing $y = \bar{y}/\delta$ with a small parameter $\delta = \tau - \tau_{H\infty}$ into (4.1), we obtain the following equations for \bar{y} and η :

$$\begin{cases} \dot{\bar{y}} = \delta\eta, \\ \dot{\eta} = g\left(\frac{\bar{y}}{\delta}, \eta; \tau\right). \end{cases} \quad (4.3).$$

For τ very closely to $\tau_{H\infty}$, the second equation in (4.3) is approximated by

$$\dot{\eta} = g(\infty, \eta; \tau), \quad (4.4)$$

where the function of $g(\infty, \eta; \tau)$ is drawn in Fig. 4.5. For $\tau > \tau_{H\infty}$, (4.4) has the unique critical point η_* (< 0) which is globally asymptotically stable (Fig. 4.5(a)). If $\eta(t_*) > 0$ for some time t_* , then $\eta(t)$ tends monotonously to η_* (< 0). This indicates that $z_R(t)$ (resp. $z_L(t)$) changes the direction and moves with asymptotically constant velocity η_* (resp. $-\eta_*$). On the other hand, for $\tau < \tau_{H\infty}$, there are two stable critical points η^* (> 0) and η_* (< 0), as shown in Fig. 4.5(c). If $y(t) > 0$, it tends to η^* (> 0), which indicates that there are no longer any periodic solutions and $z_R(t)$ (resp. $z_L(t)$) moves with asymptotically constant velocity η^* (resp. $-\eta^*$), respectively.

We note that as τ decreases, which of $\tau_{H\infty}$ and τ_{H-} first occurs depends on values of the parameter γ . In fact, when $\gamma = 0.99$, the periodic solution of (4.1) branch first disappears at $\tau = \tau_{H\infty}$, while when $\gamma = 0.9$, it first disappears at $\tau = \tau_{H-}$.

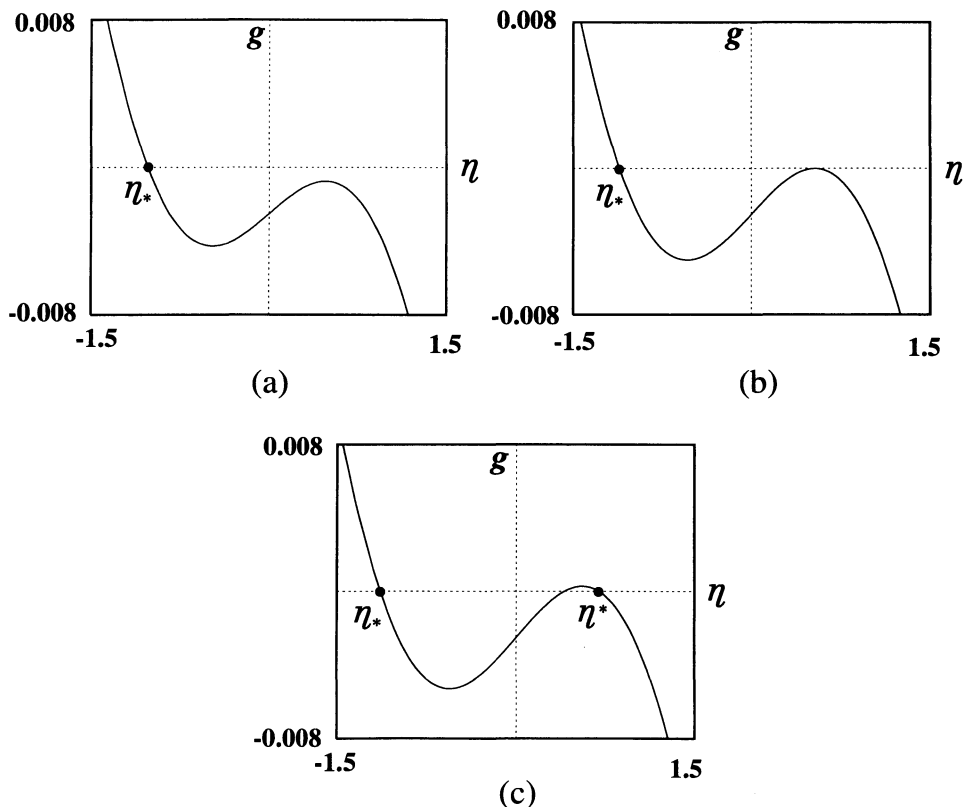


Fig. 4.5 The graph of $\dot{\eta} = g(\infty, \eta; \tau)$: (a) $\tau > \tau_{H\infty}$ ($\tau = 0.345$); (b) $\tau = \tau_{H\infty}$ ($\tau = 0.34205$); (c) $\tau < \tau_{H\infty}$ ($\tau = 0.341$).

We next consider the solution-structure of the full 3-dimensional system (3.10) when τ is varied. Here we take the SP-critical point $(0, y^*, 0)$ as the trivial solution branch, which gives the stationary interfaces $z_R = x^* + y^*$ and $z_L = x^* - y^*$ for any fixed x^* , as in Fig. 4.6. As the nonlinearities F and G in (3.10) are rather complicated, we rely on the AUTO software package [2] to know the global structure of critical points and periodic solutions when τ is varied. The structure is essentially classified into three cases, depending on values of γ .

Case I Fix γ to be very close to but less than γ^* (that is, P and R are almost odd symmetric with Q , as in Fig. 2.2). The bifurcation diagram with τ is shown in Fig. 4.7. When τ is large, $(0, y^*, 0)$ is stable. As τ decreases, it is primarily destabilized at $\tau = \tau_H$ through Hopf bifurcation so that a

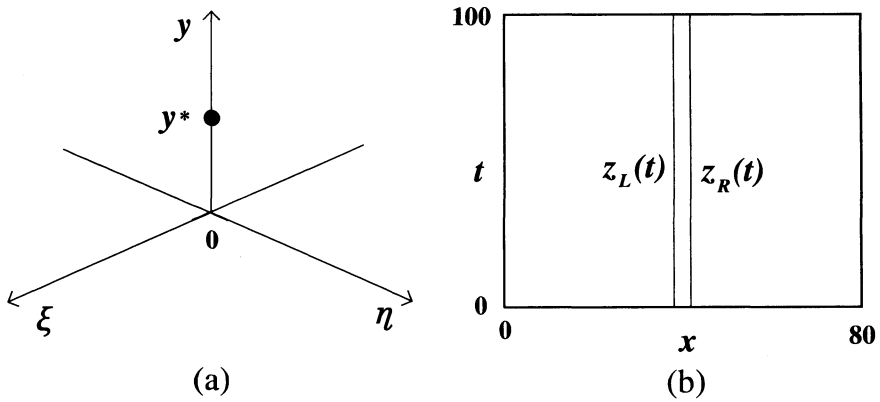


Fig. 4.6 An SP-critical point and the corresponding stationary interfaces where $a = 0.25$, $\gamma = 0.99$, $\tau = 0.39$: (a) A critical point of (3.10) in (ξ, η, y) -space; (b) standing interfaces.

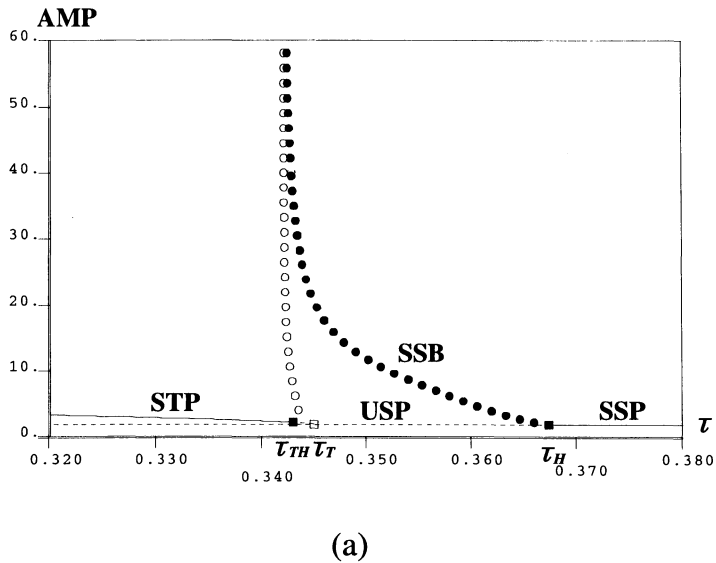
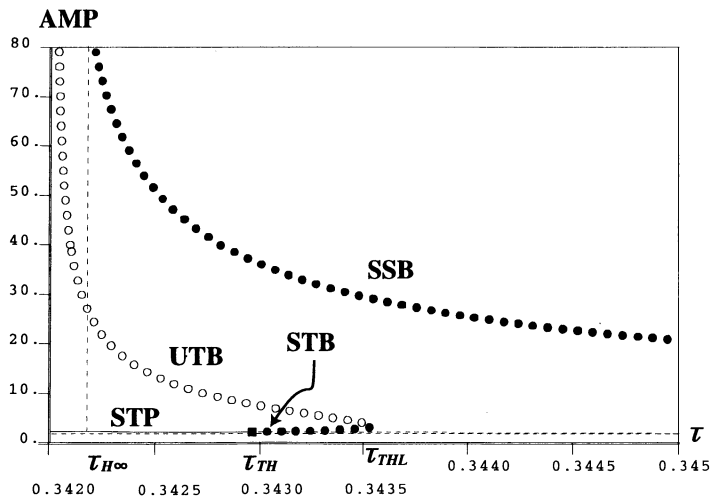
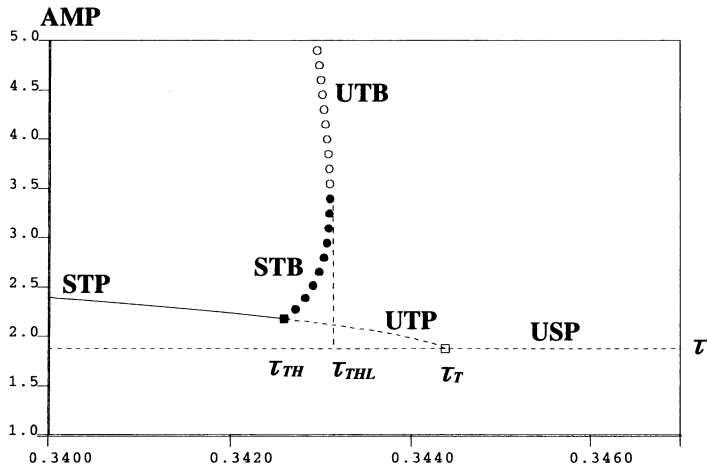


Fig. 4.7 (a) Bifurcation diagram with τ where $a = 0.25, \gamma = 0.99$ (SSP: Stable standing pulse, USP: Unstable standing pulse, STP: Stable travelling pulse, SSB: Stable standing breather, STB: Stable travelling breather, UTB: Unstable travelling breather.); (b) solution-structure near the secondary bifurcation point τ_T ; (c) solution-structure near the Hopf bifurcation point τ_{TH} .



(b)



(c)

Fig. 4.7 (continued)

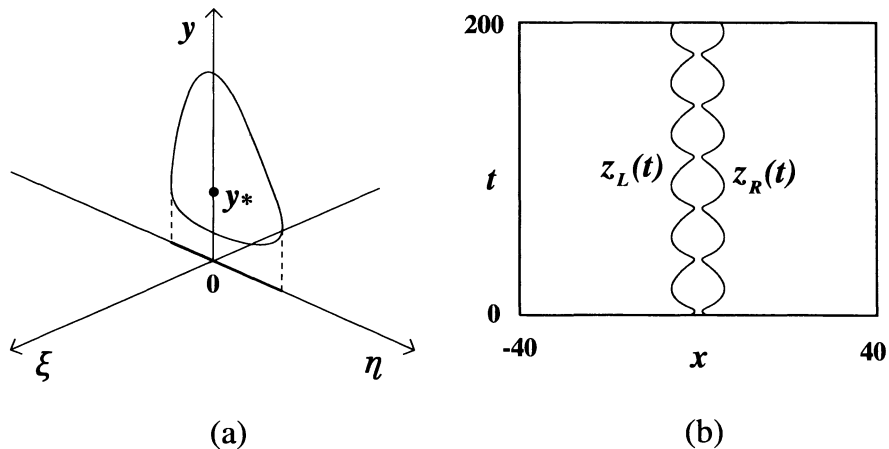


Fig. 4.8 An SB-periodic solution where the parameters are the same as Fig. 4.7 except $\tau = 0.361$: (a) Limit cycle in (ξ, y, η) -space; (b) oscillatory interfaces.

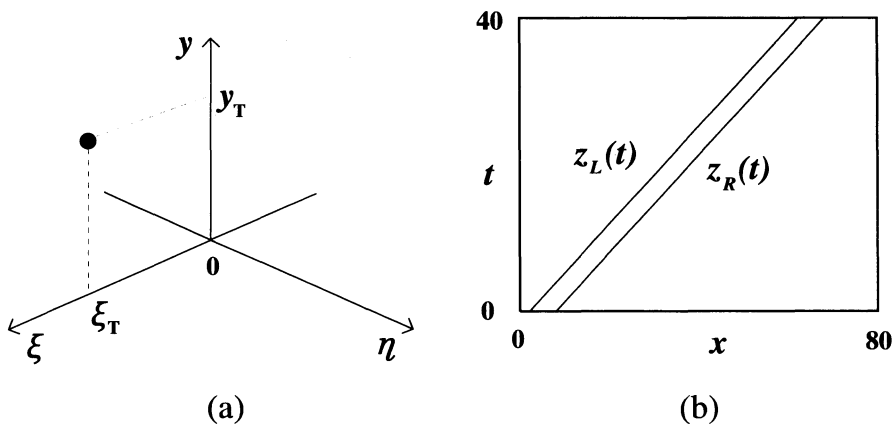


Fig. 4.9 A TP-critical point where the parameters are the same as Fig. 4.7 except $\tau = 0.32$: (a) A critical point of (3.10) in (ξ, y, η) -space; (b) travelling interfaces.

2-dimensional periodic solution $(0, y_0(t), \eta_0(t))$ super-critically bifurcates, which is a stable SB-periodic solution (Fig. 4.8). However, it disappears as τ decreases to $\tau_{H\infty}$ (Fig. 4.7(b)). A TP-critical point $(\xi_T, y_T, 0)$ bifurcates from $(0, y^*, 0)$ at $\tau = \tau_T$, but it is unstable for τ near τ_T , because it is the secondary bifurcation (Fig. 4.7(c)). There is a Hopf bifurcation at $\tau = \tau_{TH}$ so that $(\xi_T, y_T, 0)$ recovers its stability for $\tau < \tau_{TH}$ (Fig. 4.9), from which a TB-periodic solution sub-critically bifurcates.

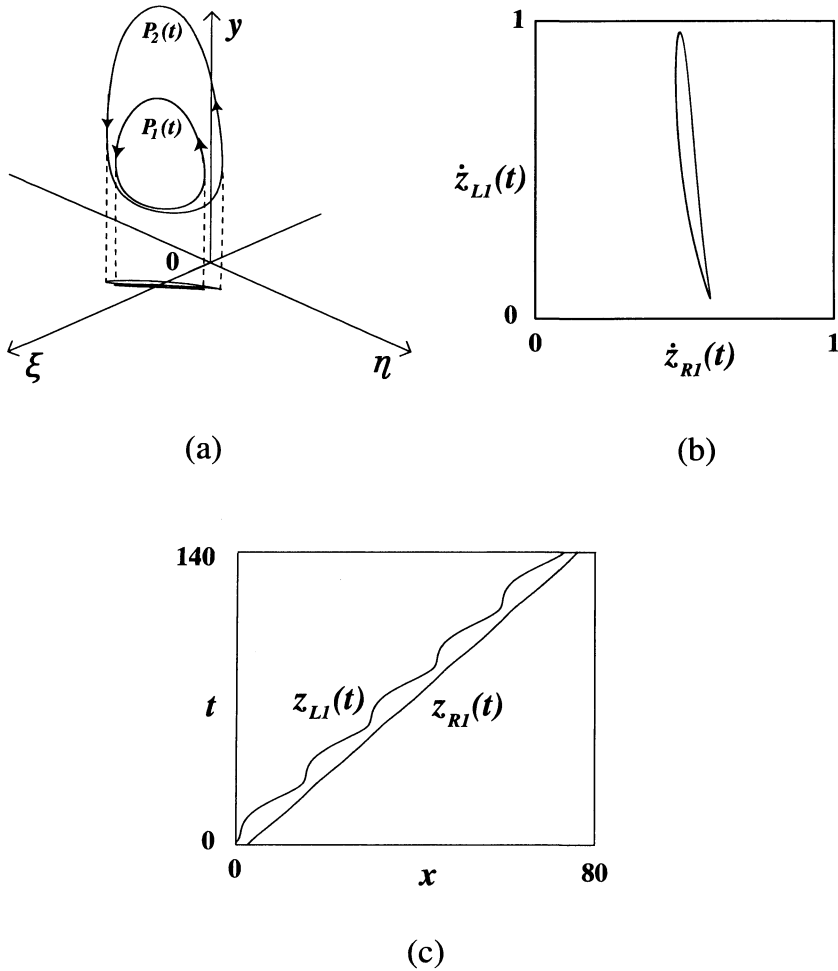
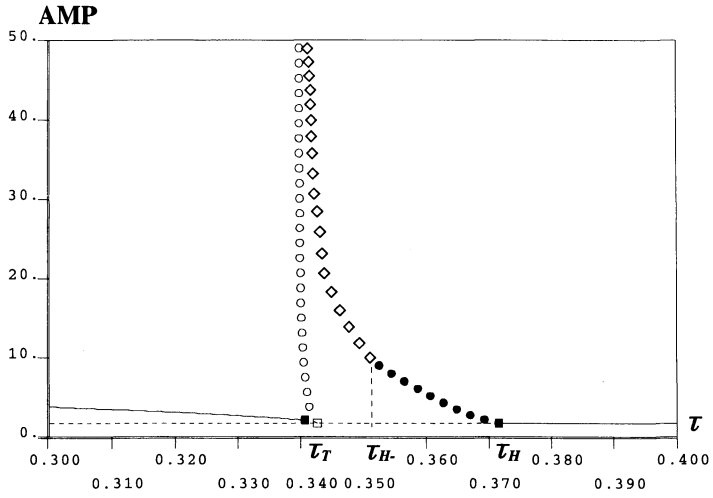
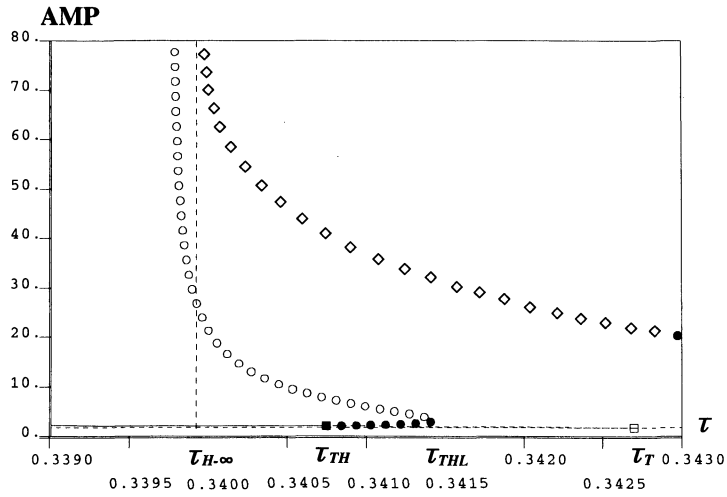


Fig. 4.10 TB-periodic solutions where the parameters are the same as Fig. 4.7 except $\tau = 0.3435$: (a) Two limit cycles $P_1(t)$ and $P_2(t)$ in the (ξ, y, η) -space; (b) The relation between $\dot{z}_{LI}(t)$ and $\dot{z}_{RI}(t)$; (c) travelling breather interfaces.

We remark that this solution branch possesses a limiting point at $\tau = \tau_{THL}$ (Fig. 4.7(c)), that is, there are *two* TB-periodic solutions $P_1(t) = (\xi_1(t), y_1(t), \eta_1(t))$ and $P_2(t) = (\xi_2(t), y_2(t), \eta_2(t))$, where $P_1(t)$ is stable, while $P_2(t)$ is unstable (Fig. 4.10(a)). The time evolutions of $z_{LI}(t)$ and $z_{RI}(t)$ corresponding to $P_1(t)$ are drawn in Figs. 4.10(b) and

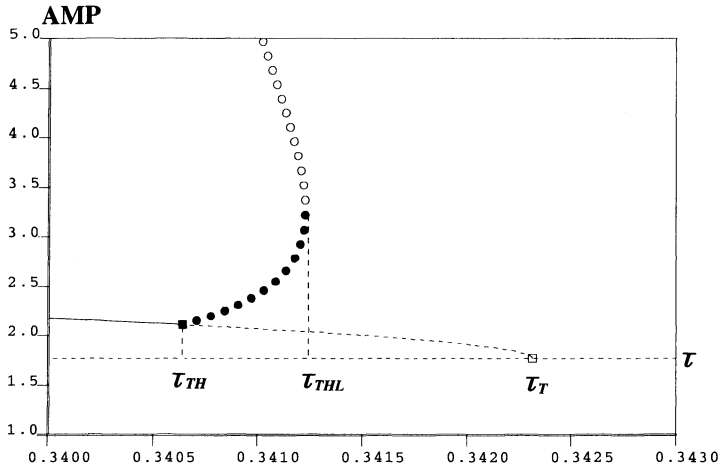


(a)



(b)

Fig. 4.11 (a) Bifurcation diagram with τ where the parameters are the same as Fig. 4.7 except $\gamma = 0.9865$; (b) solution-structure near the secondary bifurcation point τ_T ; (c) solution-structure near the Hopf bifurcation point τ_{TH} ; \diamond is periodic solution of (4.1) where $y_0(t; \tau)$ has lost its positivity.



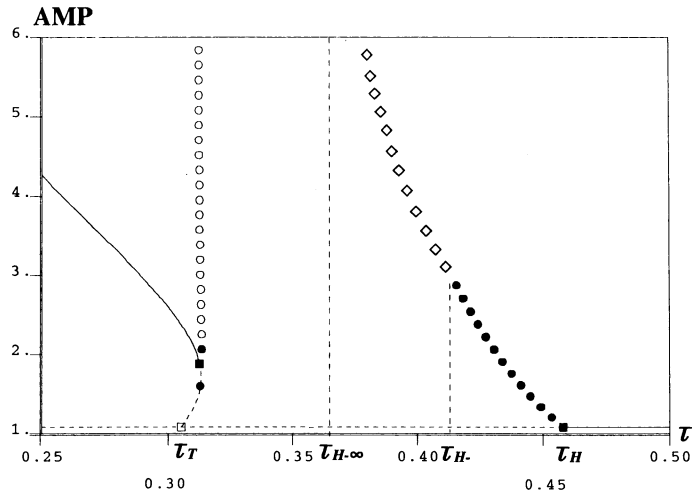
(c)

Fig. 4.11 (continued)

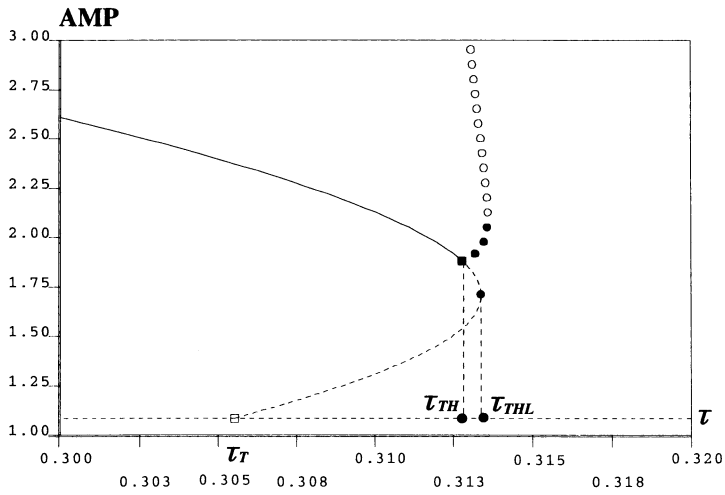
(c). One can obviously see that the velocity of $z_{R1}(t)$ is almost constant, while $z_{L1}(t)$ is clearly oscillating. This is qualitatively in good agreement with the behaviors of internal layers in RD system (2.1), (2.2) and interfaces in the limiting problem (2.3)–(2.7), as were shown in Figs. 1.2 and 2.3(d), respectively.

Case II Fix γ to be slightly smaller than the value of γ for Case I. As in Fig. 4.11, the bifurcation diagram is almost similar to Case I except that the SB-periodic solution disappears at $\tau = \tau_{H-}$ where $y(t)$ becomes zero at finite time. If we ignore the positivity of $y(t)$, the branch continues until $\tau = \tau_{H-\infty}$. It is noted that there exists some interval (τ_{THL}, τ_{H-}) where no stable solution exists.

Case III Fix γ to be slightly smaller than the value of γ for Case II. The structure is almost similar to Case II except that the TP-critical point $(\xi_0, y_0, 0)$ bifurcates *sub-critically* from $(0, y^*, 0)$ and there is a limiting point at $\tau = \tau_H$, as in Fig. 4.12.



(a)



(b)

Fig. 4.12 (a) Bifurcation diagram with τ where the parameters are the same as Fig. 4.7 except $\gamma = 0.9$; (b) solution-structure near the secondary bifurcation point τ_T .

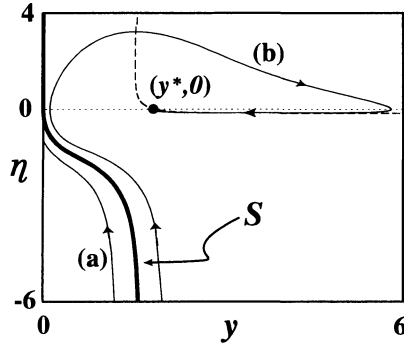


Fig. 5.1 Solution-trajectories of (4.1), depending on initial conditions where the parameters are $a = 0.25, \gamma = 0.99, \tau = 0.4$.

5. Discussion

In this section, with the help of the bifurcation diagrams obtained in Figs. 4.7, 4.11 and 4.12, we consider the dynamics of solutions of (3.10) and then give several conjectures on the dynamics of travelling breathers arising in RD system (2.1), (2.2). We take the initial condition to (3.10) as

$$\begin{cases} \xi(0) = \xi_0, \\ y(0) = y_0 > 0, \\ \eta(0) = \eta_0. \end{cases} \tag{5.1}$$

Let $z_L(t), z_R(t)$ and $v(t, x)$ be solutions of (2.3)–(2.7) for suitably fixed initial functions $z_L(0), z_R(0)$ and $v(0, t)$. For suitably small $t_* > 0$, we take the initial values ξ_0, y_0 and η_0 as

$$\xi_0 = \frac{1}{2\tau} [\lambda(v(t_*, z_R(t_*))) - \lambda(v(t_*, z_L(t_*)))],$$

$$y_0 = \frac{z_R(t_*) - z_L(t_*)}{2}$$

and

$$\eta_0 = \frac{1}{2\tau} [\lambda(v(t_*, z_R(t_*))) + \lambda(v(t_*, z_L(t_*)))],$$

respectively.

Here, we restrict our discussion to Case I (see Fig. 4.7), by which we consider the dynamics of pulse-solutions of (2.1), (2.2), depending on values of τ .

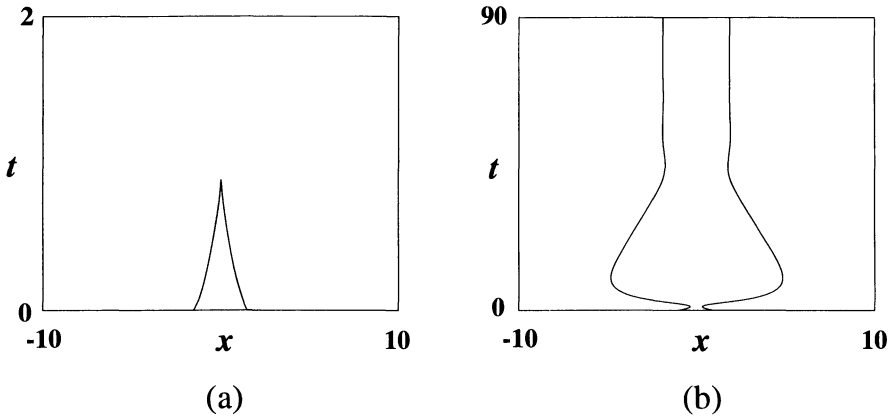


Fig. 5.2 Behavior of interfaces z_L and z_R to (4.1) in (x, t) -plane where the parameters are the same as Fig. 5.1: (a) Collision of interfaces; (b) SP-interfaces.

(i) Large τ ($\tau_H < \tau < \infty$)

In this situation, the SP-critical point $(0, y^*, 0)$ of (3.10) is asymptotically stable. We first discuss the special case when $\xi_0 = 0$. Since $F(0, y, \eta) = 0$, we may simply consider (4.1). Let the curve C be the trajectory $(y(t), \eta(t))$ of (4.1) with $(y_0, \eta_0) = (0, 0)$ for $t < 0$ and define S by $S = C \cup \{(y, \eta) \in \mathbf{R}^2 \mid y = 0, \eta > 0\}$ in $\{(y, \eta) \in \mathbf{R}^2 \mid y \geq 0, \eta \in \mathbf{R}\}$, as shown in Fig. 5.1. It turns out that when the initial value (y_0, η_0) is slightly above the curve S , any solution $(y(t), \eta(t))$ of (4.1) tends to the critical point $(y^*, 0)$, while, when $(y(0), \eta(0))$ is slightly below S , $y(t)$ of the solution tends to zero at finite time, that is, the dynamics of the interfaces $z_L(t)$ and $z_R(t)$ of (3.1) is separated into two cases, which is shown in Fig. 5.2. This information tells us the possibility of two types of dynamics of pulse-solutions in the RD system (2.1), (2.2), depending on initial conditions. The collision of $z_L(t)$ and $z_R(t)$ suggests the extinction of a pulse-solution of (2.1), (2.2) at finite time. When $\xi_0 \neq 0$, though we can no longer use the above simple argument and have to consider (3.10), we numerically confirm that the dynamics of solutions of (3.10) and the corresponding pulse-solutions of (2.1), (2.2) are similar to the above.

(ii) Intermediate τ ($\tau_{THL} < \tau < \tau_H$)

If τ satisfies $\tau_T < \tau < \tau_H$, there exist the unstable SP-critical point and the stable SB-periodic solution. As was stated in Case (i), (4.1) gives a separator S in (y, η) -plane. When the initial value (y_0, η_0) is above the curve S , any trajectory $(y(t), \eta(t))$ tends to the SB-periodic solution, while when (y_0, η_0) is

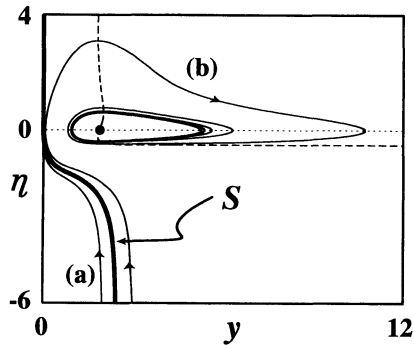


Fig. 5.3 Solution-trajectories of (4.1), depending on initial conditions where the parameters are the same as Fig. 5.1 except $\tau = 0.361$.

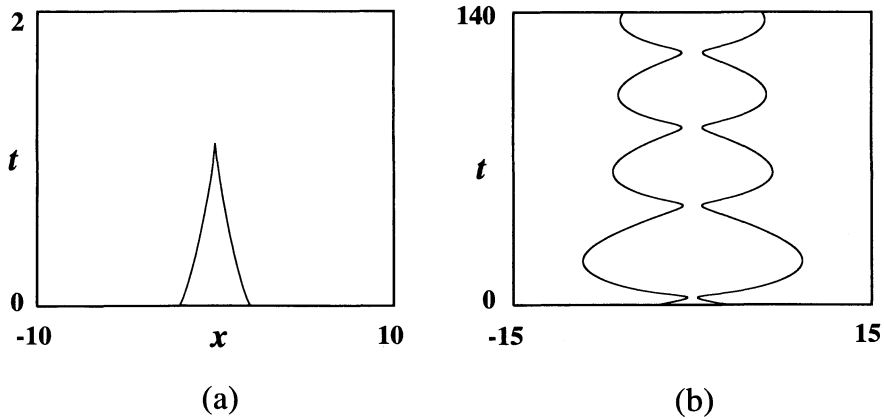


Fig. 5.4 Behavior of interfaces z_L and z_R in (4.1) on (x, t) -plane where the parameters are the same as Fig. 5.3: (a) Collision of interfaces; (b) SB-interfaces.

below S , $y(t)$ tends to zero at finite time (Fig. 5.3). Similarly to the previous case, (4.1) exhibits two types of dynamics of solutions, which are separated by S ; one is the collision of interfaces at finite time and the other is approaching to a standing breather (Fig. 5.4). When $\xi_0 \neq 0$, numerical calculation of (3.10) suggests that the dynamics of solutions is similar to the above. These behaviors are also confirmed for RD system (2.1), (2.2).

If τ satisfies $\tau_{THL} < \tau < \tau_T$ where the stable state is still the SB-periodic solution only, the situation is almost similar to the above except that the

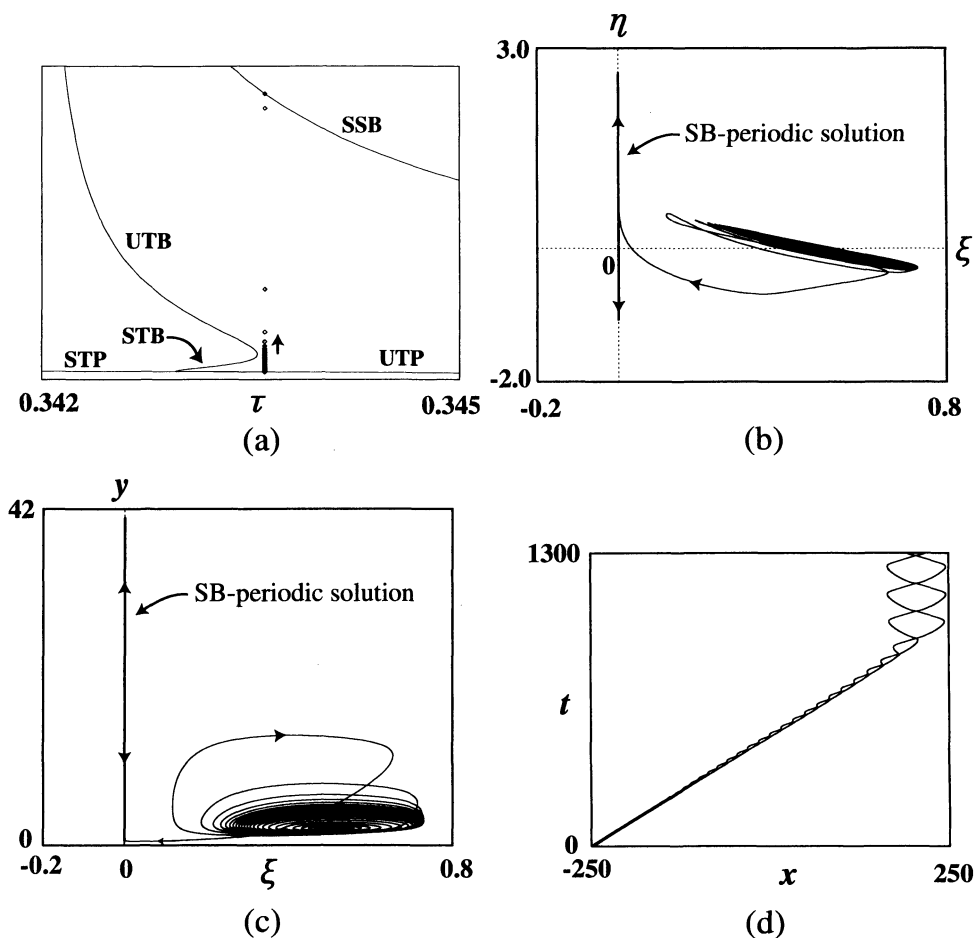


Fig. 5.5 Transition from the unstable TP-critical point to the stable SB-periodic solution in (3.10) where the parameters are the same as Fig. 5.1 except $\tau = 0.343596$: (a) A bifurcation diagram near limiting point at $\tau = \tau_{THL}$; (b) solution-trajectories in (ξ, y) -plane; (c) solution-trajectories in (ξ, η) -plane; (d) behaviors of interfaces z_L and z_R .

unstable TP-critical point exists. It is interesting to consider the case when τ is fixed to be slightly larger than τ_{THL} . Let the initial value (ξ_0, y_0, η_0) be close to the unstable TP-critical point. Then, one can expect that the solution of (3.10) tends asymptotically to the stable SB-periodic solution. However, as in Figs. 5.5(a), (b) and (c), one notices that the solution behaves as if it were a TB-periodic solution as the transient behaviour, though there is no TB-periodic solution. This can be interpreted as follows: Since τ is close to τ_{THL} , the

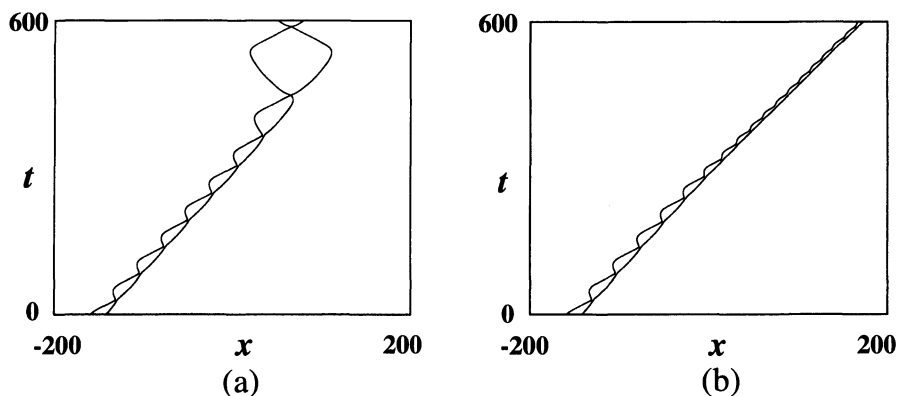


Fig. 5.6 Transition from the unstable TB-interfaces to the stable states of interfaces z_L and z_R of (3.1) where the parameters are the same as Fig. 5.1 except $\tau = 0.3432$: (a) SB-interfaces; (b) TB-interfaces.

transient behaviour of solutions is similar to that of the TB-periodic solution at $\tau = \tau_{THL}$, by the *aftereffect* of the limiting point. The behavior of the corresponding $z_L(t)$ and $z_R(t)$ is shown in Fig. 5.5(d). We recall that this behavior is qualitatively similar to the one in RD system (2.1), (2.2), which was shown in Fig. 1.5.

(iii) Slightly small τ ($\tau_{TH} < \tau < \tau_{THL}$)

This situation is rather complicated. There coexist five different types of pulse-solutions; the unstable SP- and TP-critical points, the stable SB-periodic solution, the stable and unstable TB-periodic solutions. It is numerically shown that for fixed τ , the dynamics of pulse-solutions is generically classified into three types; vanishing of $y(t)$ and approaching to either the stable SB- or the stable TB-periodic solutions. Under this situation, the unstable TB-periodic solution plays a role of separator between these two stable periodic solution, as in Fig. 5.6. This suggests the existence of two travelling breathers in (2.1), (2.2) where one is stable and the other is unstable.

(iv) Small τ ($\tau_{H\infty} < \tau < \tau_{TH}$)

In this situation, there coexist the unstable SP- and the stable TP-critical points and the stable SB- and the unstable TB-periodic solutions. In a similar way to Case (iii), we find that there are three types of dynamics of solutions; vanishing of $y(t)$ and approaching to either the SB-periodic solution or TP-critical point, as in Fig. 5.7. We find that the dynamics of pulse-solutions of (2.1), (2.2) is also classified into three types, depending on initial conditions.

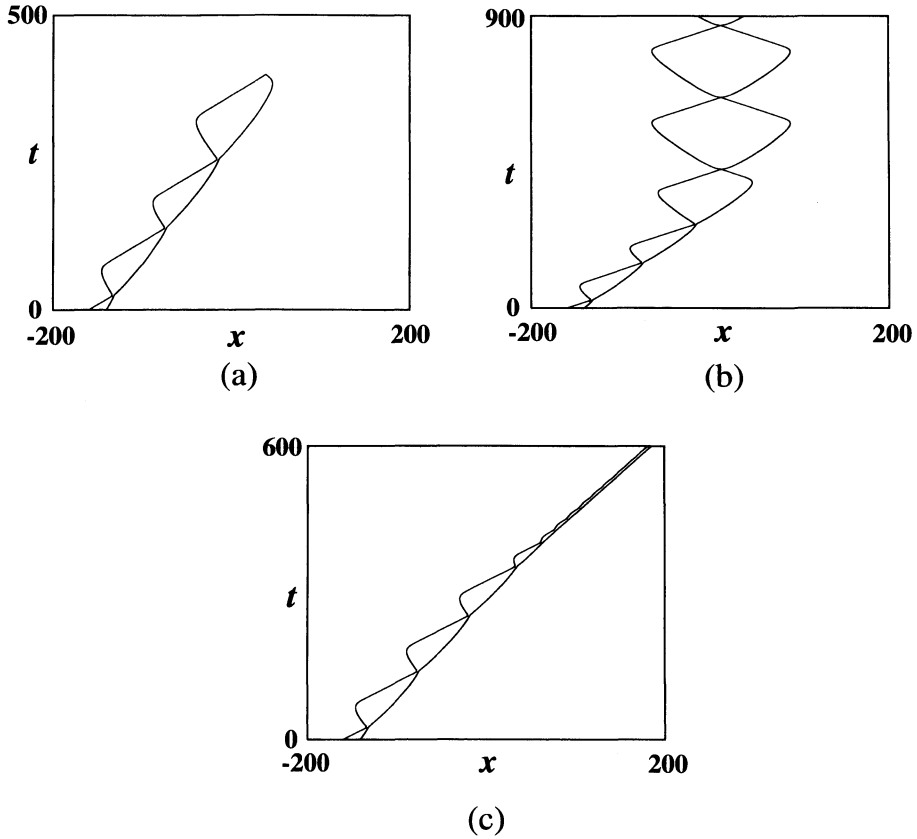


Fig. 5.7 Behaviors of interfaces z_L and z_R of (3.1) where the parameters are the same as Fig. 5.1 except $\tau = 0.3425$: (a) Collision of interfaces; (b) transition to the SB-interfaces; (c) transition to the TP-interfaces.

(v) Rather small τ ($0 < \tau < \tau_{H\infty}$)

In this situation, the structure is rather simple, that is, there is the stable TP-critical point and the unstable SP-critical point and the TB-periodic solution. The dynamics of solutions of (3.10) falls into three cases; $y(t)$ tends to either zero or infinity or to the TP-critical point, as in Fig. 5.8. Numerical simulations confirm that the dynamics of solutions of (2.1), (2.2) is also classified into three cases, depending on initial conditions.

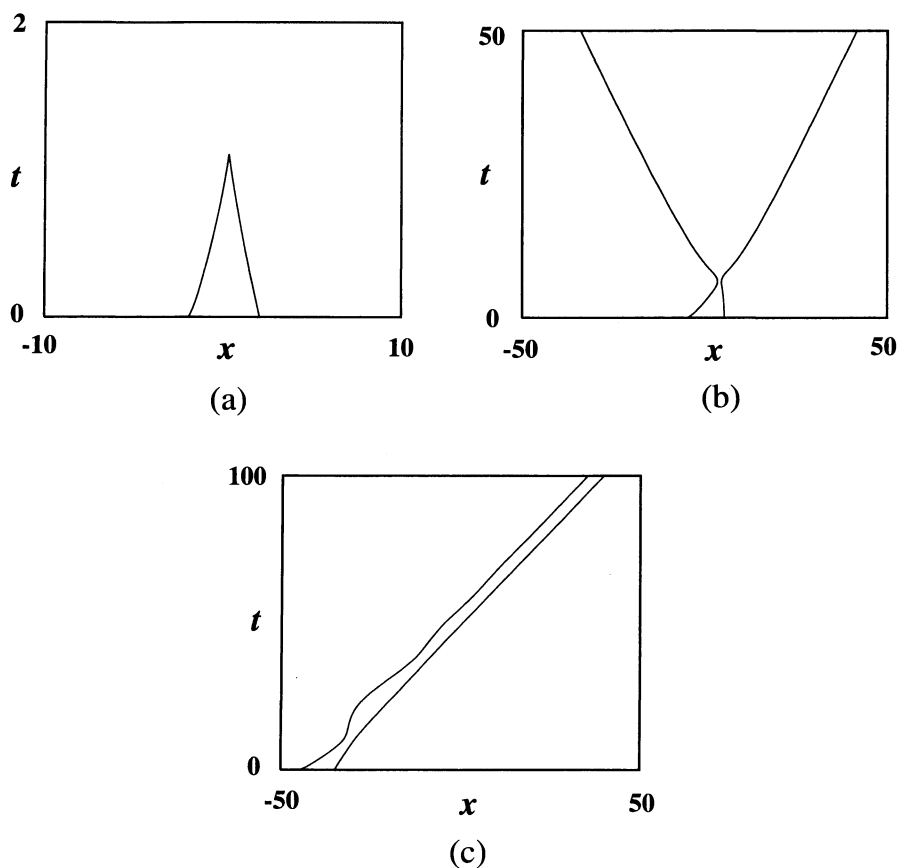


Fig. 5.8 Behaviors of interfaces z_L and z_R of (3.1) where the parameters are the same as Fig. 5.1 except $\tau = 0.342$: (a) Collision of interfaces; (b) expanding interfaces; (c) TP-interfaces.

The cases (II) and (III) are similarly discussed, so we omit them. Here we remark the dynamics of solutions of (3.10) shown in Fig. 4.11(b). Suppose τ is fixed to be slightly larger than τ_{THL} where no stable solution exists. As in Fig. 5.9, the solution $y(t)$ tends zero, but the transient behavior of solutions is as if it were a TB-periodic solution by the aftereffect of limiting point. This resembles the dynamics of pulse-solutions of (2.1), (2.2) shown in Fig. 1.4.

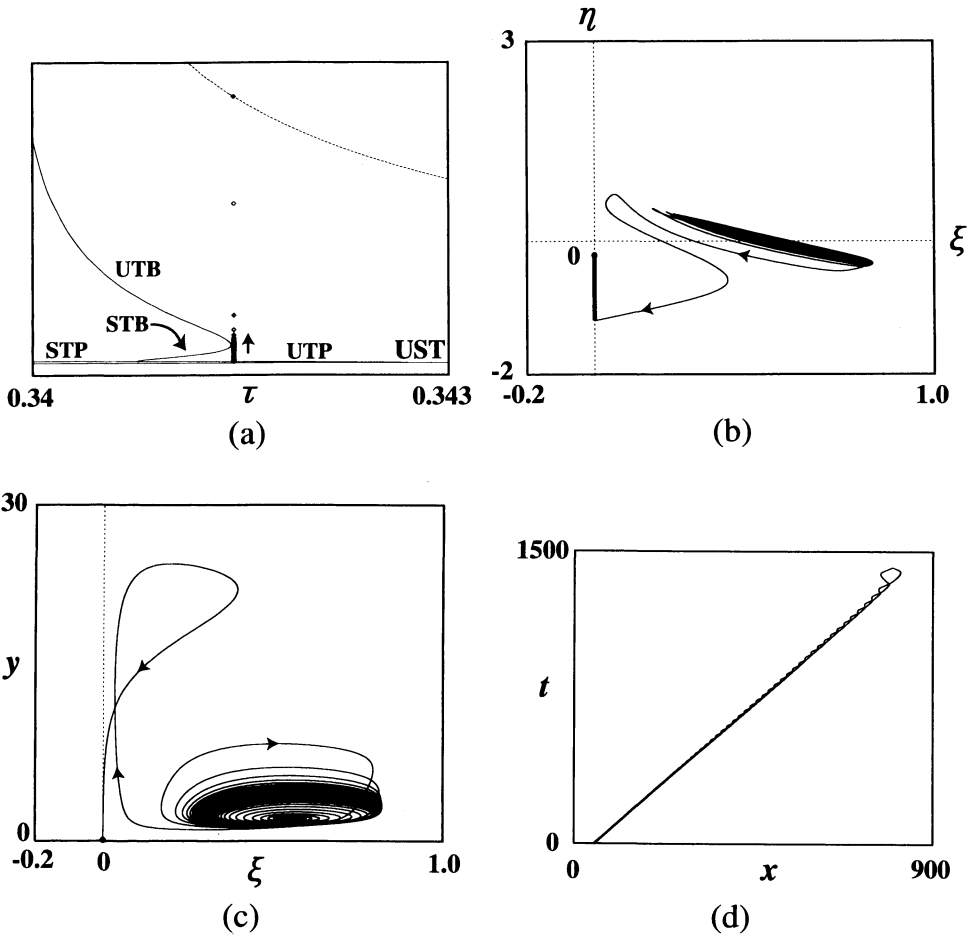


Fig. 5.9 Transition from the unstable TP-critical point to the $y(t) = 0$ solution of (3.10) where the parameters are the same as Fig. 5.1 except $\gamma = 0.9865, \tau = 0.34145$: (a) A bifurcation diagram near limiting point; (b) a solution-trajectory in (ξ, η) -plane; (c) a solution-trajectory in (ξ, y) -plane; (d) a behaviors of interfaces z_L and z_R .

6. Concluding remarks

In order to understand the dynamics of pulse-solutions of a bistable RD system with a layer parameter ε , we have derived a 4-dimensional ODEs to describe the motion of the front- and back-interfaces of pulse, taking the limit $\varepsilon \downarrow 0$. The analysis of the ODEs has enabled us to know the existence as well as stability of standing and travelling pulses, standing and travelling breathers arising in the RD system. Furthermore, when the time constant parameter τ is varied, the global structure of these pulses have been revealed. For the

derivation of the reduced ODEs, we restrict ourselves to the situation that γ is close to γ^* , that is, the pulse-length of solutions is very large. Under this situation, it is found that when τ decreases, the bifurcation point τ_H appears first and τ_T secondly does. However, we should note that when a is close to $1/2$ and γ is slightly apart from γ^* so that the pulse-length is narrow, τ_T appears first and τ_H secondly does [4]. This indicates the occurrence of codimension two singularity when $\tau = \tau_T = \tau_H$ for a suitable value of γ . We thus expect the existence of more complicated structures of pulse-solutions of the RD system. Unfortunately, our reduced ODEs can not be applied to this situation. We should need to develop any other tools to investigate it. This is a future work for us.

Acknowledgments

We have benefited from discussions with Takao Ohta on the derivation of ODEs describing interfaces in Section 3.

7. Appendix

Appendix A

We formally derive the ODEs (3.1) from (2.3) and (2.5). When $f(u) = H(u - a) - u$, the free boundary problem (2.3)–(2.7) can be rewritten as follows:

$$\frac{\tau \dot{z}_R(t)}{\sqrt{(\tau \dot{z}_R(t))^2 + 4}} = 1 - 2a - 2v(t, z_R(t)), \quad t > 0, \tag{A.1}$$

$$\frac{\tau \dot{z}_L(t)}{\sqrt{(\tau \dot{z}_L(t))^2 + 4}} = -1 + 2a + 2v(t, z_L(t)), \quad t > 0 \tag{A.2}$$

and

$$\begin{cases} \frac{\partial v}{\partial t} = \frac{\partial^2 v}{\partial x^2} - (1 + \gamma)v, & t > 0, \quad x \in \mathbf{R} \setminus (z_L(t), z_R(t)), \\ \frac{\partial v}{\partial t} = \frac{\partial^2 v}{\partial x^2} + 1 - (1 + \gamma)v, & t > 0, \quad x \in (z_L(t), z_R(t)) \end{cases} \tag{A.3}$$

with the boundary condition

$$\lim_{|x| \rightarrow \infty} v(t, x) = 0, \quad t > 0 \tag{A.4}$$

and the regularity condition

$$v(t, \cdot) \in C^1(\mathbf{R}), \quad t > 0. \tag{A.5}$$

Applying the Fourier transform given by

$$v_q(t) = \int_{-\infty}^{\infty} v(t, x) e^{iqx} dx$$

to (A.3), we have

$$\dot{v}_q(t) = -(q^2 + \beta)v_q(t) + \frac{1}{iq} (e^{iqz_R(t)} - e^{iqz_L(t)}), \tag{A.6}$$

where $\beta = 1 + \gamma$. The inverse Fourier transform of (A.6) yields

$$\begin{aligned} v(t, x) &= \frac{1}{2\pi} \int_{-\infty}^{\infty} \frac{1}{iq} \int_0^t \exp(-(q^2 + \beta)(t - s) - iqx) e^{iqz_R(s)} ds dq \\ &\quad - \frac{1}{2\pi} \int_{-\infty}^{\infty} \frac{1}{iq} \int_0^t \exp(-(q^2 + \beta)(t - s) - iqx) e^{iqz_L(s)} ds dq. \end{aligned} \tag{A.7}$$

by ignoring the term $v_q(0) \exp(-(q^2 + \beta)t)$, since we consider the dynamics after large time. Hence we obtain

$$\begin{aligned} v_1(t) &= v(t, z_R(t)) \\ &= \frac{1}{2\pi} \int_{-\infty}^{\infty} \frac{1}{iq} \int_0^t \exp(-(q^2 + \beta)(t - s) - iqz_R(t)) e^{iqz_R(s)} ds dq \\ &\quad - \frac{1}{2\pi} \int_{-\infty}^{\infty} \frac{1}{iq} \int_0^t \exp(-(q^2 + \beta)(t - s) - iqz_R(t)) e^{iqz_L(s)} ds dq \end{aligned} \tag{A.8}$$

and

$$\begin{aligned} v_2(t) &= v(t, z_L(t)) \\ &= \frac{1}{2\pi} \int_{-\infty}^{\infty} \frac{1}{iq} \int_0^t \exp(-(q^2 + \beta)(t - s) - iqz_L(t)) e^{iqz_R(s)} ds dq \\ &\quad - \frac{1}{2\pi} \int_{-\infty}^{\infty} \frac{1}{iq} \int_0^t \exp(-(q^2 + \beta)(t - s) - iqz_L(t)) e^{iqz_L(s)} ds dq. \end{aligned} \tag{A.9}$$

(A.8) and (A.9) indicate that there is a time-delayed interaction between two interfaces mediated by v . Therefore, in order to take account of the effect of the time-delayed interaction in (A.8) and (A.9), we employ the following expansion:

$$z_i(s) = z_i(t) + \dot{z}_i(t)(s - t) + \ddot{z}_i(t) \frac{(s - t)^2}{2} + \dots \quad (i = R, L). \tag{A.10}$$

After straightforward calculation, we approximate (A.8) ignoring the 3rd and higher derivatives [8]

$$v_1(t) = v_1^{(1)}(t) + v_1^{(2)}(t), \quad (\text{A.11})$$

where

$$\begin{aligned} v_1^{(1)}(t) &= \frac{1}{2\pi} \int_{-\infty}^{\infty} \frac{2}{2iq} \left(\frac{1}{q^2 + \beta + iq\dot{z}_R} - \frac{\exp(-iq(z_R - z_L))}{q^2 + \beta + iq\dot{z}_L} \right) dq \\ &= \frac{1}{2\beta\phi_R} \phi_{R-} - \frac{1}{2\beta\phi_L} \phi_{L-} \exp\left(- (z_R - z_L) \frac{\phi_{L+}}{2}\right), \end{aligned} \quad (\text{A.12})$$

where $\phi_i = \phi(\dot{z}_i) = \sqrt{z_i^2 + 4\beta}$ and $\phi_{i\pm} = \phi_i \pm z_i$ ($i = L, R$), and

$$v_1^{(2)}(t) = \frac{1}{2\pi} \int_{-\infty}^{\infty} \left(\frac{1}{(q^2 + \beta + iq\dot{z}_R)^3} \ddot{z}_R - \frac{\exp(-iq(z_R - z_L))}{(q^2 + \beta + iq\dot{z}_L)^3} \ddot{z}_L \right) dq. \quad (\text{A.13})$$

In the above representation of $v_1(t)$ in (A.11), the term of $O(\exp(-\beta t))$ was ignored, since we consider the dynamics after large time. From (A.9), we may derive the representation of $v_2(t) = v_2^{(1)}(t) + v_2^{(2)}(t)$ in the similar way to (A.12) and (A.13) where

$$\begin{aligned} v_2^{(1)}(t) &= \frac{1}{2\pi} \int_{-\infty}^{\infty} \frac{2}{2iq} \left(-\frac{1}{q^2 + \beta + iq\dot{z}_L} + \frac{\exp(iq(z_R - z_L))}{q^2 + \beta + iq\dot{z}_R} \right) dq \\ &= \frac{1}{2\beta\phi_L} \phi_{L+} - \frac{1}{2\beta\phi_R} \left(\phi_{R+} \exp(-(z_R - z_L) \frac{\phi_{R-}}{2}) \right), \end{aligned} \quad (\text{A.14})$$

and

$$-v_2^{(2)}(t) = \frac{1}{2\pi} \int_{-\infty}^{\infty} \left(\frac{1}{(q^2 + \beta + iq\dot{z}_L)^3} \ddot{z}_L - \frac{\exp(iq(z_R - z_L))}{(q^2 + \beta + iq\dot{z}_R)^3} \ddot{z}_R \right) dq. \quad (\text{A.15})$$

Thus one may write $v_1^{(2)}$ and $v_2^{(2)}$ as

$$v_1^{(2)} = m(z_R, \dot{z}_R) \ddot{z}_R - n_1(z_R, z_L, \dot{z}_L) \ddot{z}_L \quad (\text{A.16})$$

and

$$-v_2^{(2)} = m(z_L, \dot{z}_L) \ddot{z}_L - n_2(z_R, z_L, \dot{z}_R) \ddot{z}_R, \quad (\text{A.17})$$

respectively, where

$$m(z_i, \dot{z}_i) = \frac{1}{2\pi} \int_{-\infty}^{\infty} \frac{1}{(q^2 + \beta + iq\dot{z}_i)^3} dq = \frac{6}{\phi_i^5} \quad (i = L, R). \quad (\text{A.18})$$

In a similar way to (A.12), n_1 and n_2 are defined by

$$\begin{aligned}
 n_1 &= \frac{1}{2\pi} \int_{-\infty}^{\infty} \frac{\exp(-iq(z_R - z_L))}{(q^2 + \beta + iq\dot{z}_L)^3} dq \\
 &= \left(\frac{(z_R - z_L)^2}{2\phi_L^3} + \frac{3(z_R - z_L)}{\phi_L^4} + \frac{6}{\phi_L^5} \right) \exp(-(z_R - z_L)\phi_{L+}), \quad (\text{A.19})
 \end{aligned}$$

$$\begin{aligned}
 n_2 &= \frac{1}{2\pi} \int_{-\infty}^{\infty} \frac{\exp(iq(z_R - z_L))}{(q^2 + \beta + iq\dot{z}_R)^3} dq \\
 &= \left(\frac{(z_R - z_L)^2}{2\phi_R^3} + \frac{3(z_R - z_L)}{\phi_R^4} + \frac{6}{\phi_R^5} \right) \exp(-(z_R - z_L)\phi_{R-}). \quad (\text{A.20})
 \end{aligned}$$

Therefore (3.1) can be obtained.

Appendix B

We show that the stability of $(x^* + \xi_T t, \xi_T, y_T, 0)$ and $(x^* + \int_0^t \xi_0(s) ds, \xi_0(t), y_0(t), \eta_0(t))$ solutions of the 4-dimensional ODE system (3.6) is given by the stability of SP- and TP-critical points and SB- and TB-periodic solutions of the 3-dimensional ODE systems (3.10), respectively.

PROPOSITION 7.1. *If the TP-critical point $(\xi_T, y_T, 0)$ of (3.10) is exponentially stable, then $(x^* + \xi_T t, \xi_T, y_T, 0)$ of (3.6) is also exponentially stable.*

PROOF. Since the TP-critical point is exponentially stable, there exist some constants a_1 and $a_2 > 0$, such that

$$|\xi(t) - \xi_T| \leq a_1 e^{-a_2 t}.$$

Therefore there exists some constant h_0 such that

$$\lim_{t \rightarrow +\infty} \int_0^t (\xi(s) - \xi_T) ds = h_0.$$

By using $\dot{x} = \xi$, one easily knows that

$$x(t) - x(0) - \xi_T t = \int_0^t (\xi(s) - \xi_T) ds,$$

which leads

$$\lim_{t \rightarrow \infty} [x(t) - (x^* + \xi_T t)] = [x(0) - x^* + h_0] = h,$$

this gives the proof.

In a similar way to Proposition 7.1, we obtain

PROPOSITION 7.2. *If the TB-periodic solution $(\xi_0(t), y_0(t), \eta_0(t))$ of (3.10) is exponentially stable, then $(x^* + \int_0^t \xi_0(s) ds, \xi_0(t), y_0(t), \eta_0(t))$ of (3.6) is also exponentially stable.*

References

- [1] M. Bar, M. Hildebrand, M. Eiswirth, M. Falcke, H. Engel and M. Neufeld, Chemical turbulence and standing waves in a surface reaction model: The influence of global coupling and wave instabilities, *Chaos* **4**(3), 1994, 499–508.
- [2] E. Doedel, H. B. Keller and J. P. Kernevez, Numerical analysis and control of bifurcation problems (I) Bifurcation in finite dimensions, *Int. J. Bifurcation and Chaos* **1**, 1991, 493–520.
- [3] H. Ikeda and T. Ikeda, Bifurcation phenomena from standing pulse solutions in some reaction-diffusion systems, *J. Dynamics and Differential Equations* **12**, 2000, 117–167.
- [4] T. Ikeda, H. Ikeda and M. Mimura, Hopf bifurcation of travelling pulses in some bistable reaction-diffusion systems, to appear in *Methods and Applications of Analysis*.
- [5] M. Mimura and M. Nagayama, Nonannihilation dynamics in an exothermic reaction-diffusion system with mono-stable excitability, *Chaos* **7**(4), 1997, 817–826.
- [6] M. Mimura, M. Nagayama and T. Ohta, Nonannihilation of travelling pulses in reaction-diffusion systems, to appear in *Methods and Applications of Analysis*.
- [7] J. Nagumo, S. Arimoto and S. Yoshizawa, An active pulse transmission line simulating nerve axon, *Proc. IRE* **50**, 1962, 2061–2070.
- [8] T. Ohta, J. Kiyose and M. Mimura, Collision of propagating pulse in a reaction-diffusion system, *J. Phys. Soc. Japan* **66**, 1997, 1551–1558.
- [9] J. Pearson, Complex patterns in a simple system, *Sciences* **261**, 1993, 189–192.
- [10] V. Petrov, S. K. Scott and K. Showalter, Excitability, wave reflection, and wave splitting in a cubic autocatalysis reaction-diffusion systems, *Phil. Trans. Roy. Soc. Lond.* **A347**, 1994, 631–642.
- [11] J. J. Tyson and P. C. Fife, Target patterns in a realistic model of the Belousov-Zhabotinskii reaction, *J. Chem. Phys.* **73**(5), 1980, 2224–2237.
- [12] X.-F. Chen, Generation and propagation of interfaces in reaction-diffusion systems, *Trans. Amer. Math. Soc.* **334**, 1992, 877–913.

M. Mimura

*Department of Mathematical and Life Sciences,
Graduate School of Science
Hiroshima University
Higashi-Hiroshima 739-8526, Japan*

M. Nagayama

*Research Institute for Mathematical Sciences
Kyoto University
Kyoto 606-8502, Japan*

H. Ikeda

*Department of Mathematics
Toyama University
Toyama 930-8555, Japan*

T. Ikeda

*Department of Applied Mathematics and Informatics
Ryukoku University
Ohtsu 520-2194, Japan*